

# The Benchmark Greenium

This version: March 31, 2023

## **Abstract**

Exploiting the unique “twin” structure of German government green and conventional securities, we use a dynamic term structure model to estimate a sovereign risk-free greenium, distinct from the yield spread between the green security and its conventional twin (i.e., the green spread). The model purifies the green spread from pecuniary factors unrelated to environmental preferences. While the model-implied greenium exhibits a significant relation with proxies of shocks to climate concerns—and the green spread does not—the green spread correlates with stock market prices and measures of flight-to-quality. We also estimate the full greenium term structure and expected green returns.

Keywords: ESG, green bonds, dynamic no-arbitrage models  
JEL Classifications: G12, Q51

# 1 Introduction

According to recent estimates, investments of \$5 trillion per year are needed by 2030 to meet climate goals compatible with the Paris Climate Agreement (World Resource Institute, 2021).<sup>1</sup> Mobilizing public and private financial resources is key to generating the trillions of dollars needed for the rapid transition required. Governments can play an important role in setting the right incentives and policies to steer finances away from emission-intensive (brown) projects and toward environmentally-sustainable (green) projects. One possible way is to lead by example and issue sovereign green bonds, that is, government-guaranteed bonds whose proceeds are exclusively used to fund adaptation and mitigation projects.

In this study, we estimate the benchmark greenium, the premium specific to risk-free green securities relative to otherwise identical non-green securities. Such a greenium can serve as a reference point to price the greenium in other green assets. Correctly identifying the benchmark greenium is important because it reveals the subsidy investors are willing to provide the government to finance the green transition. In other words, the greenium we want to capture is a convenience yield investors are willing to pay beyond the expected risk and return characteristics of the green security and is unrelated to pecuniary motives. Overall, the benchmark greenium measures savings to governments that shift their expenditures from brown to green projects, and it can provide a justification for central banks to include safe green bonds in the conduct of conventional and unconventional monetary policy.

The type of greenium that interests us—and that arguably is of interest to policy makers, investors, and researchers alike—is not directly observable from government security prices. However, the relatively new German federal green securities provide us with a natural experiment that facilitates the estimation of the greenium for three reasons. First, German government securities are considered among the safest in the world, so much so that, for most of the last decade, their yields have been negative even at long maturities. Second, in Germany, environmental and climate protection has been a top priority for several years. This has been clearly emphasized once again in the Climate Change Act 2021, in which the federal government committed to being climate neutral by 2045. This commitment translates into a credible promise to allocate green securities’ proceeds only to green projects (i.e., low fungibility risk). Finally, the German Finance Agency (GFA) has designed the green security to attenuate as much as possible concerns regarding, for instance, lack of liquidity, reporting transparency, and reliable green ratings.

Specifically, to issue green federal securities the GFA uses a novel “twin” structure: each

---

<sup>1</sup>Alternative estimates are even larger: 2018 OECD estimates are of \$6.9tr per year and UN IPCC \$2.4tr per year in the energy sector alone.

green security is the twin of a conventional security, which has identical cash-flows and maturity but whose proceeds are not earmarked to finance green projects. In principle, the yield spread between the green security and its conventional twin (the green spread) should reflect only the greenium. This is because, for each pair of twin securities, the conventional yield should “control for” all factors affecting German sovereign yields except for the factor associated to climate/environmental concerns. However, it is clear from Figure 1, which plots the green spread and the German stock market index, that the green spread is inversely related to stock prices and hence it is likely contaminated by pecuniary motives.

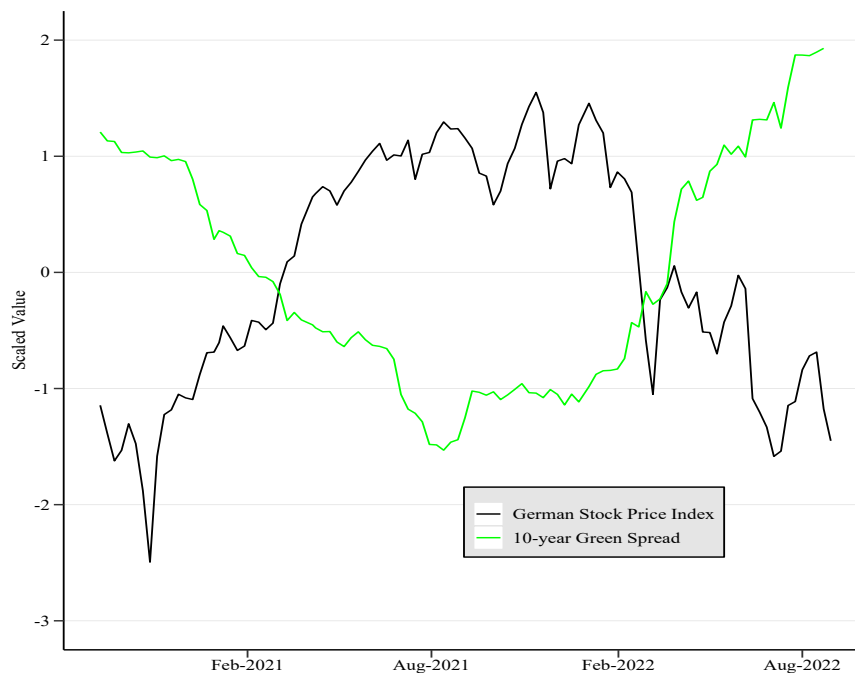


**Figure 1.** Relation between the Green Spread and Stock Prices

The green line depicts the yield spread between the first green security and its conventional twin issued by the German government in September 2020 and the black line depicts the normalized series for the German Stock Price Index (DAX).

Figure 1 suggests that risk factors unrelated to investors’ environmental preferences can drive a wedge between the observable green spread and the underlying benchmark greenium. These risk factors consist of both confounding factors, common to all pairs of twins, that result in demand/supply imbalances between green and conventional securities (e.g., transitory flight-to-quality episodes), and idiosyncratic factors specific to the particular pair of twins used to construct the green spread (e.g., issuance size and dates).<sup>2</sup> Both types of factors, being unrelated to economic fundamentals (among which damages from environmental

<sup>2</sup>Each green security and its conventional twin are issued a few months apart and in different amounts.

disasters), cause *temporary* mispricing of the greenium. And, this mispricing should be more relevant in the early years of green securities, as their supply ramps up, and in crisis periods when concerns about climate protection take a back seat.

To purge green spreads from the relative mispricing induced by idiosyncratic and confounding factors, we introduce a dynamic no-arbitrage term-structure model (DTSM) that jointly prices German nominal green and conventional securities. The security-level DTSM extends [Pancost \(2021\)](#) to back out a set of conventional factors that price all conventional and green securities outstanding, in addition to a “green” factor specific to green bonds only. The green factor captures the price component related to environmental/climate concerns, that is, the dividend investors are willing to forego to subsidize green projects. We estimate daily conventional and green factors from the panel of prices of all outstanding federal green and conventional securities, which provides dynamic estimates of green and conventional yield curves. The difference between these two yield curves provides a benchmark greenium at every maturity—a greenium term structure.

Beyond purging the greenium estimates from confounding and idiosyncratic factors, using a DTSM has two additional advantages. First, the model delivers time-varying estimates of the greenium, which in turn allows us to analyze the drivers of its fluctuations. This is key to test whether the model-implied greenium and green spreads are driven by different risk factors. Second, our DTSM allows us to obtain ex-ante expected green and conventional returns and compare them to the realized ones. This makes us well equipped to assess whether investors choose green assets because of their expected performance relative to brown assets or because of non-pecuniary reasons. Green spreads alone offer no estimate of expected future returns. The equilibrium model of [Pastor, Stambaugh and Taylor \(2021\)](#) predicts that green assets should have lower expected returns than brown assets, and our DTSM allows us to empirically test this prediction for government green bonds.

We have three main findings. First, the model-implied greenium often differs from the observed green spread: it tends to be significantly larger, varying between 0 and 8 basis points; at times it moves in the opposite direction of the green spread (widening while the green spread is narrowing); and its term structure is upward-sloping rather than downward-sloping as in the green spread. Second, proxies of confounding factors, such as stock market prices, measures of flight-to-quality and liquidity, do not affect the model-implied greenium, but do correlate with the green spread. Conversely, the benchmark greenium does respond to shocks to environmental concerns, such as jumps in oil prices and the economic damages from environmental disasters—which in our sample are mainly driven by the devastating German floods in the summer of 2021. Interestingly, once we control for confounding factors, the green spread does not react significantly to shifts in environmental concerns.

Third, the estimated expected green excess return (i.e., the difference between expected green and conventional returns) varies with the investment horizon and investors' information set, as it is positive at issuance (September 2020) and turns negative after the German floods (July 2021). In line with Pastor, Stambaugh and Taylor (2021), as investors become more concerned about the environment, they are willing to accept lower returns to hold green assets. This is consistent with a widening greenium, which implies a larger subsidy to the government to finance green projects. Further, as suggested by Pastor, Stambaugh and Taylor (2022), the expected and realized green excess returns diverge when there is an unanticipated increase in climate concerns; but, they diverge also when there are surprises unrelated to environmental preferences, such as the start of the Ukrainian war that triggered flight-to-quality to German conventional securities. This finding is consistent with a green spread that, differently from the greenium, is contaminated by confounding risk factors. In our sample, while shocks to climate concerns trigger unexpected inflows into green securities causing them to perform better than expected, shocks to risk attitude trigger unexpected inflows into their conventional twins causing green securities to perform worse than expected.

Our work has been informed by different strands of the literature. First, Pastor, Stambaugh and Taylor (2021) and Zerbib (2022) show mechanisms through which environmental preferences can generate a "taste" premium in green stocks, and motivate our search for the greenium. Second, Pastor, Stambaugh and Taylor (2022), despite being focused on the US stock market, are the first to use German twin bonds to illustrate the widening of the green spread during periods of heightened climate concerns.

Third, our paper is closely related to several empirical studies assessing the value of green bonds relative to otherwise similar non-green bonds. They show that the greenium estimates in mostly municipal and corporate green bonds vary greatly: from zero (Larcker and Watts (2020)), to relatively small (-6 bps in Baker et al. (2018) and -2 bps in Zerbib (2019)), to sizable (-63 bps in Colombage and Nanayakkara (2020)). Further, Karpf and Mandel (2018), Flammer (2020), Flammer (2021), Kapraun et al. (2021), and Berg et al. (2021) highlight factors different from environmental preferences that affect greenium estimates, such as issuance size, creditworthiness and credibility of the issuer, and noise in ESG ratings. Differently from all these studies, we focus on German sovereign bonds, as we aim to obtain a risk-free dynamic estimate of the greenium and its term structure. Importantly, having a DTSM allows us to obtain a time-varying greenium and analyze the drivers of its fluctuations, and to study ex-ante expected green returns, which makes us well equipped to test the theory of Pastor, Stambaugh and Taylor (2021) for government green bonds.

More broadly, our research also relates to the literature investigating the pricing of climate change in financial markets; although, we are not focused on analyzing financial instruments

that are linked to or hedge climate risks (e.g., Engle et al. (2020), Alekseev et al. (2021), Chikhani and Renne (2022)). Like Zerbib (2019), our premise is that the greenium, being related to environmental preferences, should not be driven by pecuniary motives, such as hedging financial losses due to climate change. On the contrary, the greenium that we isolate is a dividend that investors are willing to forgo to fund mitigation and adaptation projects, providing a subsidy to the government.

Still, our paper has been shaped by the growing work on how climate change risks are priced in financial markets. For instance, Bansal, Kiku and Ochoa (2016) find that the risk of climate change (proxied by rising temperature) negatively affects asset valuations. Bernstein, Gustafson and Lewis (2019) and Giglio et al. (2021) price climate risk in the real estate market. Similarly, Painter (2020) finds a climate risk premium in the primary US municipal bond market and Huynh and Xia (2021) in the corporate bond market. In the case of derivatives, Ilhan, Sautner and Vilkov (2021) estimate a climate tail risk premium. Finally, Bauer and Rudebusch (2021) provide evidence on the rising cost of climate change in the US Treasury market, while Kling et al. (2020) and Cevik and Jalles (2022) find that climate change vulnerability and resilience, as measured by the ND-GAIN index, affect sovereign bond yields and spreads.

In addition, some of our results touch on the literature focused on the investment horizon of ESG investors, which relates to the horizon of climate risk and its materialization (e.g., Starks, Venkat and Zhu (2017) and Krueger, Sautner and Starks (2020)). The upward sloping term structure of our estimated greenium might depend on the horizon of the government’s climate goals, which will require increasing green investments to transition to net zero emissions by 2045.

Finally, estimating the greenium has important policy implications. Semmler et al. (2021) show that green bonds can be useful financial instruments in fiscal policies for a transition to a low-carbon economy. Papoutsis, Piazzesi and Schneider (2021) and Riedler and Koziol (2021) analyze central banks’ portfolio allocations toward green and brown assets in the conduct of unconventional monetary policy. Oehmke and Opp (2022) support the view that more regulations are beneficial to counteract climate risk exposure, especially in the banking sector. We add to this literature by showing that the sovereign greenium is sizable enough to provide savings for governments that choose to focus on green projects, and that central banks should include safe green securities in the conduct of monetary policy, as it would make them more appealing in periods of crisis, improving their liquidity relative to conventional securities and stabilizing the greenium.

The remainder of the paper is organized as follows. Section 2 provides background information on the green bond market and the main features of the German green federal

securities. Section 3 describes the data and outlines our model and its estimation. Section 4 discusses the estimates of the greenium and its drivers. Section 5 analyzes expected and realized green excess returns. Finally Section 6 offers concluding remarks.

## 2 Green Bond Market

The green bond market is growing rapidly, and Germany is at the forefront. Green bonds are a subset of ESG investing and are the largest category of ESG fixed income, with \$620 billion issued in 2021 (about 40% of the total ESG issuance), reaching a cumulative amount of \$1.8 trillion worldwide since the inception of the green bond market in 2008 (according to Bloomberg NEF data).

Germany is the second-largest issuer of sovereign green bonds. The top panel of Figure 2 plots cumulative public issuance of green bonds over time for the nine countries that are the largest issuers and for supranational entities, such as the European Union (EU) and World Bank. The European Union (EU) is expected to dominate the green bond supply following its entrance in the market in the last quarter of 2021, as it is committed to issue up to \$225 billion by the end of 2026.

Nevertheless, green bonds remain a relatively limited component of the sovereign bond universe. In particular, as shown in the bottom panel of Figure 2, green bonds typically comprise only 1-4% of outstanding bonds even for the most prolific green issuers.

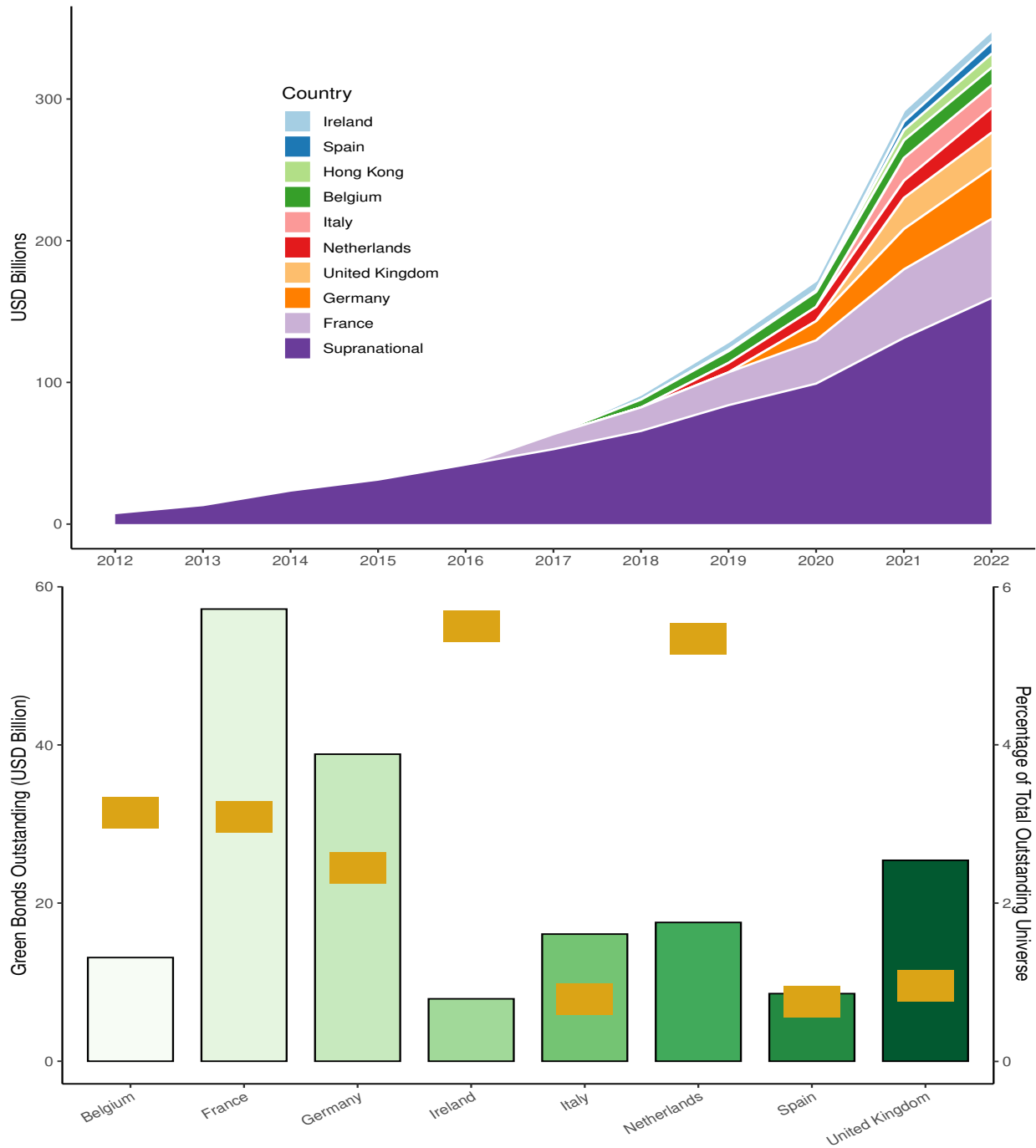


**Figure 2.** Cumulative Public Green Bond Issuance

The top panel plots cumulative public green bond issuance in billions of dollars per year. The bottom panel plots total sovereign green bond issuance in billions of dollar for the most prolific issuers and as percentage of the total debt outstanding (yellow rectangles). (Source: Bloomberg NEF).



## 2.1 German Green Federal Securities

Germany issued its first green sovereign bond in September 2020, and since then its green securities have accounted for 3 percent of the total issuance volume of German government securities. A month prior to the first issuance, ISS ESG, one of the world’s leading rating agencies in the field of sustainable investment, awarded Germany a rating of B and classified it as PRIME, on a rating scale from A+ (excellent) to D- (poor). According to ISS ESG, “as of August 21, 2020, this rating puts Germany in place 12 out of 124 countries rated by ISS ESG. This equates to a high relative performance, with a decile rank of 1.”<sup>3</sup>

Demand for German green bonds tends to be high. The first three green bonds were more than six times over-subscribed, and all four green bonds have subsequently been re-opened to increase their initial issuance. The investor base for green securities is quite broad, with real money investors accounting for the largest share. In particular, at the 10- and 30-year syndicates, asset managers, central banks, as well as insurance and pension funds acquired between 75 and 90 percent of the issuance.

German green federal securities provide an ideal testing ground for estimating the greenium for numerous reasons. First, because German debt is risk-free, security cash-flows are known with certainty and therefore any price differential between green and brown securities must represent a difference in discount rates. In contrast, greenium estimates in virtually any other asset class (corporate bonds, municipal bonds, equities) are potentially combining a difference in discount rates with a difference in cash-flows. For example, one explanation for the higher expected returns on ESG stocks found in some studies (Pastor, Stambaugh and Taylor, 2021; Berg et al., 2021) is that green companies are expected to do better in the future, either due to higher demand for green products (electric cars, for example) or due to heightened regulatory risk for brown companies (climate regulation, for example). Neither of these issues pertain to German federal securities.

Second, every green bond issued by the GFA is paired with a conventional “twin” bond with the exact same maturity date and coupon structure. Thus, not only are green-bond payments risk-free, they also occur on the exact same day as the payments from another bond whose issuance proceeds are *not* tied to green investments. The yield spread between a green bond and its conventional twin is thus an indirect—albeit imperfect, see below—

---

<sup>3</sup>ISS ESG “assesses alignment with external principles (e.g. the ICMA Green/Social Bond Principles), analyses the sustainability quality of the assets and reviews the sustainability performance of the issuer themselves. Following these three steps, we draw up an independent SPO so that investors are as well informed as possible about the quality of the bond/loan from a sustainability perspective.” For more detail on the certificate see <https://www.bundesfinanzministerium.de/Content/EN/Standardartikel/Topics/Priority-Issues/Climate-Action/green-german-federal-securities-restricted/2020-11-18-second-party-opinion-certificate.pdf>.

measure of the greenium. Table 1 lists some salient characteristics of the four German green securities and their conventional twins.

ISIN	Issue Date	Maturity	Coupon	Amount (Bil \$)	Green
DE0001102507	2020-06-19	2030-08-15	0	35.2	0
DE0001030708	2020-09-09	2030-08-15	0	8.81	1
DE0001141828	2020-07-10	2025-10-10	0	27.5	0
DE0001030716	2020-11-06	2025-10-10	0	5.51	1
DE0001102481	2019-08-23	2050-08-15	0	33.6	0
DE0001030724	2021-05-18	2050-08-15	0	6.61	1
DE0001102564	2021-06-18	2031-08-15	0	32.5	0
DE0001030732	2021-09-10	2031-08-15	0	7.16	1

**Table 1.** German Twin Bonds

This table lists all German sovereign green bonds and their respective twins. The pairs exhibit matching maturity dates and are all zero-coupon. The USD amount issued is the total amount outstanding. The last column indicates whether the bond is green (1) or conventional (0).

Third, the GFA is committed to ensuring that the green bond trades at least as liquidly as its conventional twin. Liquidity differences between bonds can be of first-order importance for understanding spreads (D’Amico, Kim and Wei, 2018), and the fact that green bond issuances are substantially smaller than their corresponding twins (Table 1), combined with the novelty of the instrument, may make green bonds less liquid. The GFA employs two tools to allay fears that the smaller green securities trade at a discount with respect to the conventional bond in the secondary market. First, the GFA allows switch trades, that is, the option to convert a green bond into the conventional twin without penalty at any time, and second, it can execute green repos, that is, temporary purchases of a green bond if its price falls below the conventional twin price’s (implicit floor).<sup>4</sup>

Fourth, the proceeds of German green bonds are more transparently allocated than other green securities, allaying concerns of “fungibility.” The auditing firm Deloitte conducts an external audit to verify the actual allocation of issue proceeds to green expenditures. Afterwards, the federal government provides two reports to the public: an allocation report linking final green expenditures to last year’s green bond issuance, and one year later an impact report detailing the impact of green spending on the environment and climate.<sup>5</sup>

<sup>4</sup>For more detail see <https://www.deutsche-finanzagentur.de/en/institutional-investors/federal-securities/green-federal-securities/>

<sup>5</sup>For more detail see <https://www.deutsche-finanzagentur.de/en/institutional-investors/federal-securities/green-federal-securities/>

Finally, Germany’s green bond issuance costs are non-recurrent, making issuance less costly and time consuming than the issuance of green bonds by private corporations. Many of the elements of the certification process outlined above occur mainly at the country rather than at the bond level. Furthermore, many of these costs are fixed, in the sense that they do not need to be borne again were the issue to be re-opened—and in fact, three of the four green bonds have been re-opened at least once.

## 2.2 German Federal Environmental Investments

Germany was making substantial green investments before issuing green securities (12.3 billion euros in 2019). Its total green bond issuance from September 2020 until June 2022 accumulates to 31 billion euros and therefore makes a very significant contribution to the total German budget used for environmental projects. In 2020 and 2021 together, the German government indicatively spent 30.3 billion euros in green investments.

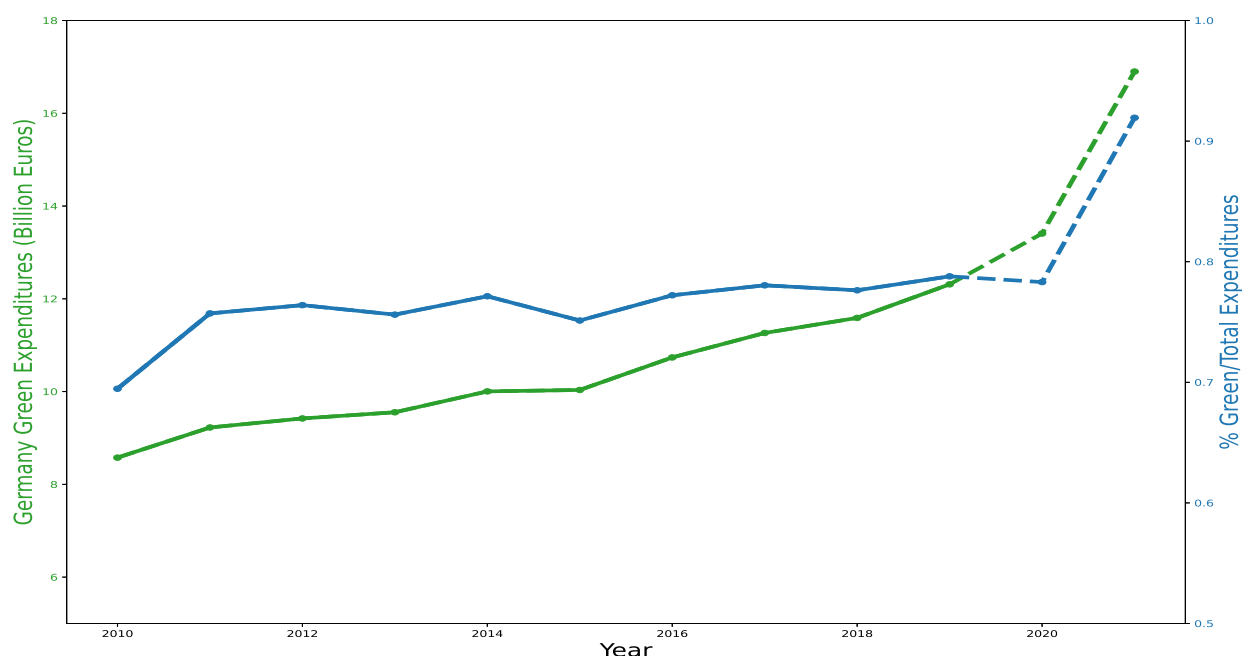


**Figure 3.** German Green Expenditures 2010-2021

The figure plots the German government expenditures on environmental projects between 2010 and 2021. The green line is the amount in billions of euros and the blue line captures the percentage of environmental investments as a fraction of total German state expenses. The numbers in 2020 and 2021 are indicative and not yet consolidated and therefore plotted with dots.

Figure 3 plots Germany’s expenses on environmental projects since 2010 in both billions securities/green-federal-securities/

of euro (green line) and as a fraction of total government spending (blue line). Green expenditures have been increasing steadily and are projected to accelerate.

The Green Bond Framework lists five main green expenditure categories that can be assigned to the green federal securities: transport; international cooperation; research, innovation and awareness raising; energy and industry; and agriculture, forestry natural landscapes and biodiversity. So far, between 50% and 55% of the expenditures has been allocated to sustainable transportation, such as rail, public and non-motorised transport, electro-mobility and alternative fuels (especially hydrogen), as transport-related emissions should be cut significantly by 2030. Between 8% and 15% of the expenditures has been allocated to the energy and industry sectors, as Germany aims for full decarbonisation by 2045 through a gradual transformation of the energy supply towards more renewable energies and energy efficiency. About 20% has been used for international cooperation, that is, mostly funding programs and projects targeted at mitigating and adapting to climate change, transitioning towards sustainable energy systems based primarily on renewable energy sources, protecting habitats and biodiversity. Finally, 8% has been used for research and about 5% for sustainable agriculture (e.g., sustainable farming, conservation and sustainable management of forests and timber use, avoiding food waste).<sup>6</sup>

### 3 Data and Model

The key features of the German green and conventional bonds are retrieved from Refinitiv Eikon. The data comprises the issue date, maturity date, coupons, their frequency, and a tag that indicates whether the bond is green or not. Eikon provides the green label to bonds that were verified by the Climate Bond Initiative (CBI), who created industry-specific standards for bond proceeds to be considered green and in line with the goals outlined in The Paris Climate Agreement. Certified third-party verifiers use the Climate Bond Taxonomy as a benchmark to assess the eligibility of a bond.<sup>7</sup> Our pricing data is from Factset; we observe 166,680 daily prices for 163 German bonds (including four green bonds) from October 27, 2008 to August 30, 2022.

---

<sup>6</sup>See slide 25 of [Deutsche Finanzagentur \(2022\)](#), available [here](#).

<sup>7</sup>Details on the verification process can be found [here](#).

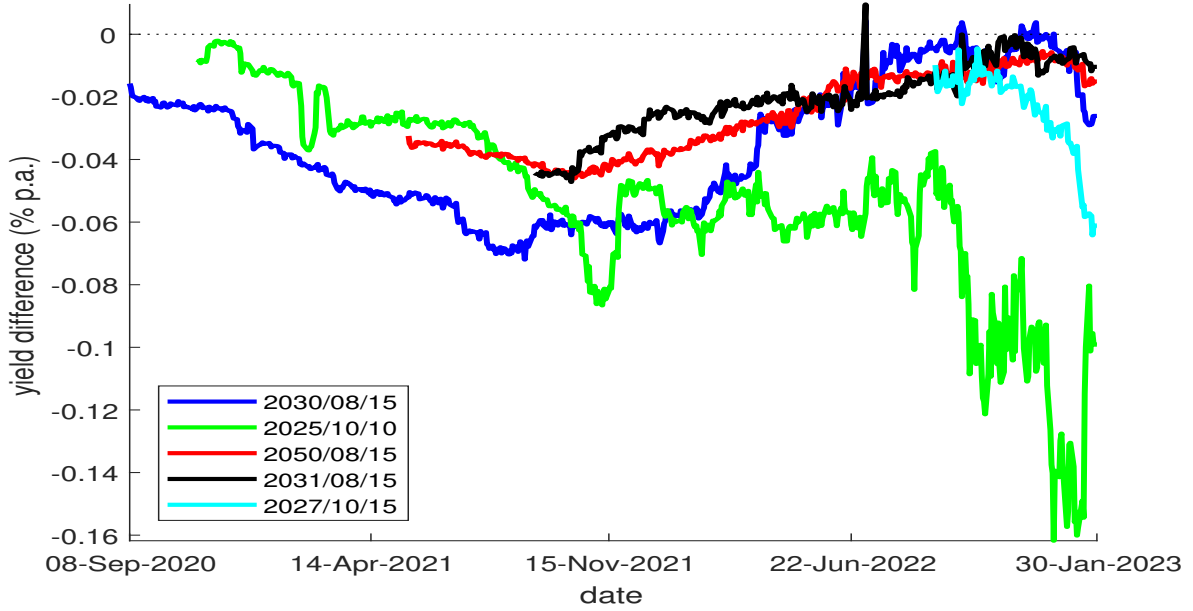


**Figure 4.** German Green Spreads

The figure plots the yield differences  $Y_{i,t}^g - Y_{i,t}$  for four pairs of German sovereign bonds. Each pair has the same coupon structure and maturity date, but one of the bonds in each pair is a certified “green” bond, whose cash-flows are earmarked for sustainable investments.

Figure 4 plots the sovereign yield spread between each of the four pairs of green and conventional twin bonds (i.e., the green spread). This setup is as close as it gets to a natural experiment due to the unique twin structure of the bonds explained in Section 2.1.

Despite the advantages of the novel “twin” structure for the identification of the greenium, the green spread is still contaminated by factors unrelated to investors’ environmental preferences, for two reasons. First, each green spread relies on a single pair of bonds, meaning it ignores the information contained in the other pairs of twins and in the full term structure of German securities. Hence, any factors specific to the particular bonds in a given pair—for instance, differences in the issuance size and dates—will contaminate the green spread. We call these factors “idiosyncratic” factors. A clear example of the importance of the idiosyncratic factors is the difference between the blue and black lines in Figure 4. Both depict green spreads that had an original maturity of 10 years but have been issued one year apart. In principle, they should convey similar information on the greenium given that they have a very similar maturity, but they do not.

Second, the green spread can be contaminated with risk factors common to all pairs of twins but unrelated to economic fundamentals, which include also expected and unexpected damages from environmental disasters. For instance, any short-lived episode that causes demand/supply imbalances between green and conventional securities might affect the green

spread but has nothing to do with environmental preferences. On the one hand, stronger demand at auctions for green bonds combined with their smaller issuance size can make these bonds scarcer than conventional bonds. On the other hand, the ECB’s purchases of large amounts of conventional bonds, as well as the flight-to-quality to those bonds, may induce conventional bonds to be scarcer than green bonds. We call these factors “confounding” factors. Both idiosyncratic and confounding factors can cause temporary mispricing of the greenium.

More formally, let  $Y_t^g$  be the yield on a riskless, constant-maturity green bond at time  $t$ , and let  $Y_t$  be the yield on an otherwise-identical conventional bond. Let  $i$  denote a particular twin pair, so that  $Y_{i,t}^g$  is the yield on the green bond and  $Y_{i,t}$  the yield on its conventional twin. Then the green spread for pair  $i$  can be written as

$$\begin{aligned}
Y_{i,t}^g - Y_{i,t} &= (Y_t^g + \tilde{\varepsilon}_{i,t}^g) - (Y_t + \tilde{\varepsilon}_{i,t}) \\
&= [(Y_t^{*g} + \tilde{\varepsilon}_t^g) + \tilde{\varepsilon}_{i,t}^g] - [(Y_t^* + \tilde{\varepsilon}_t) + \tilde{\varepsilon}_{i,t}] \\
&= \underbrace{Y_t^{*g} - Y_t^*}_{\text{fundamental greenium}} + \underbrace{\tilde{\varepsilon}_t^g - \tilde{\varepsilon}_t}_{\text{confounding factors}} + \underbrace{\tilde{\varepsilon}_{i,t}^g - \tilde{\varepsilon}_{i,t}}_{\text{idiosyncratic factors}}
\end{aligned} \tag{1}$$

where  $\tilde{\varepsilon}_{i,t}^g$  and  $\tilde{\varepsilon}_{i,t}$  are the idiosyncratic factors affecting only the two bonds in the pair  $i$ , and  $\tilde{\varepsilon}_t^g$  and  $\tilde{\varepsilon}_t$  are the additional confounding factors common to all pairs of twins. In equation (1),  $Y_t^g - Y_t$  would be the green spread purged of the purely bond-specific idiosyncratic factors; it still differs from the fundamental greenium  $Y_t^{*g} - Y_t^*$  because of the confounding factors.

To purge our estimates of the greenium from the relative mispricing induced by idiosyncratic and confounding factors, we introduce a DTSM framework that jointly prices German nominal green and conventional securities. Figure 5 illustrates how our approach differs from simply computing the green spread for a pair of “twin” securities. The figure plots conventional and green model-implied zero-coupon yield curves as red and green dotted lines, respectively, on two dates: July 15 2021 and April 19, 2022. It also shows each conventional bond outstanding as a black dot and each green bond outstanding as a green cross. Because each curve is constructed using all available bond prices, the greenium at any given maturity—given by the difference between the red and green dotted lines—is free of any idiosyncratic factors. In addition, because the model prices bonds only according to their “cash flows”—including green benefits which are non-pecuniary in nature—it is free of most confounding factors as well. However, in the next section, when we formally introduce the identification assumptions used in the model, we will discuss the advantages and limitations of such identification.<sup>8</sup>

---

<sup>8</sup>Unfortunately our setup does not allow us to separate the idiosyncratic factors  $\tilde{\varepsilon}_{i,t}^g - \tilde{\varepsilon}_{i,t}$  from the

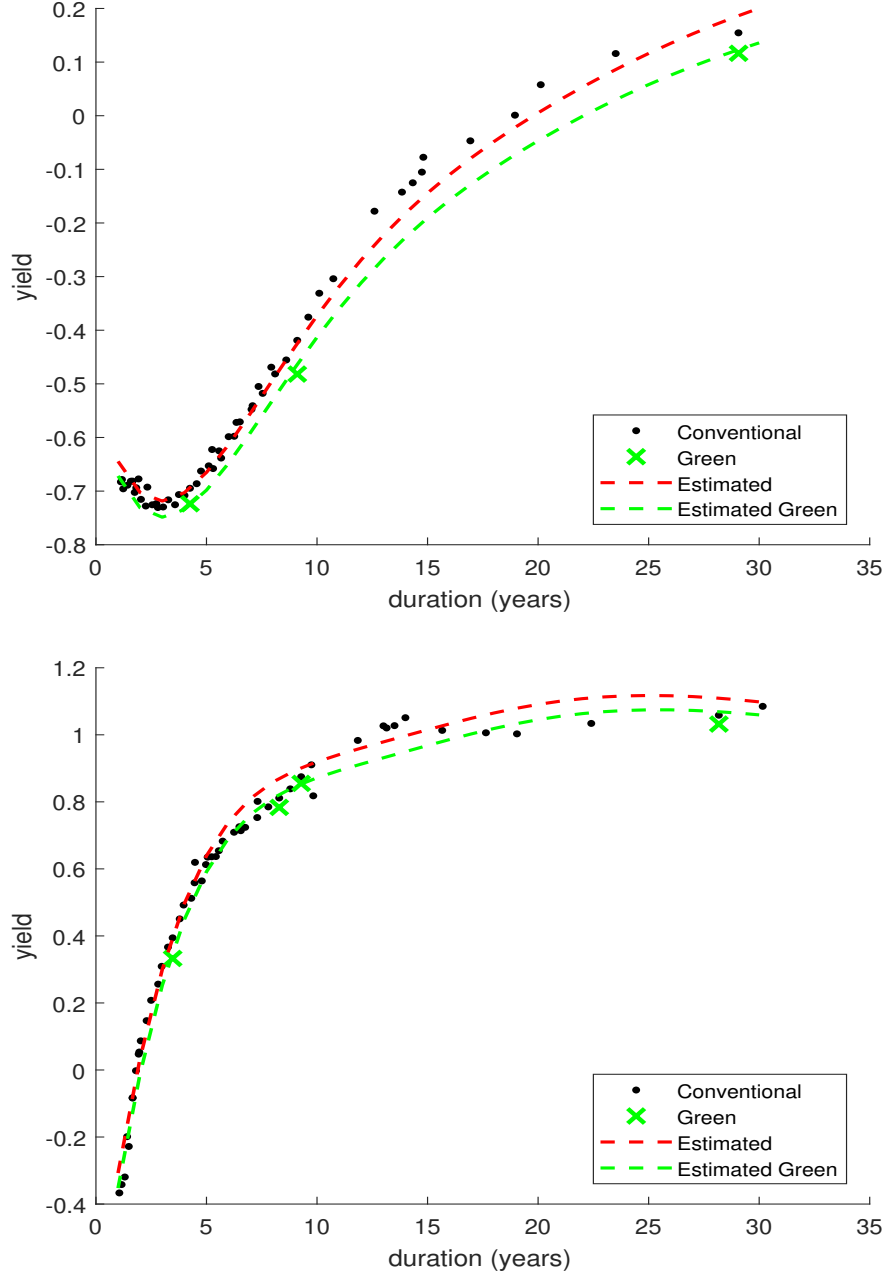


**Figure 5.** Term Structure of Greenium on Two Dates

The figure plots yields-to-maturity against duration for conventional German sovereign bonds as black dots; the four green bonds are marked in the figure as green X's. The red dotted line is the model-implied conventional zero-coupon yield curve on that day, while the green line is the model-implied green zero-coupon yield curve. The top panel plots yields on July 15, 2021; the bottom panel on April 19, 2022.

Importantly, the model described in the next section is not merely a yield-curve-fitting  


---

 confounding factors  $\tilde{\varepsilon}_t^g - \tilde{\varepsilon}_t$  in equation (1), though this would be an interesting question for future research.

exercise; it will price conventional and green securities dynamically according to a time-series model of both conventional and green discount rates. In particular, investors will price both types of bonds, at all maturities, on a given date by forecasting the time path of both green and conventional discount rates into the future. Relative to the conventional discount rate, the green discount rate is driven by an extra pricing factor, that is, the green factor, which is identified by prices differences between green and conventional bonds in the cross-section. And importantly, the model considers all conventional prices when forming the conventional yield curve, allowing it generate the relative “mispricings” of the conventional twins that are evident in Figure 5 at the long end of the yield curve. Hence, in purifying the green spread from the relative mispricing of green and conventional securities, it is not just the mispricing of green bonds that matters, but also the mispricing of the conventional twin bonds.

### 3.1 Model

We assume that the prices of Treasury bonds depend on a  $k \times 1$  vector  $X_t$  that consists of latent factors, which evolve according to an Ornstein-Uhlenbeck process:

$$dX_t = \left[ -\mu_x - \phi_x X_t \right] dt + \Sigma_x dW_t^x, \quad (2)$$

where  $W_t^x$  is a standard Brownian motion, and  $\mu_x$ ,  $\phi_x$ , and  $\Sigma_x$  are parameters to be estimated.

In order to price green bonds, we assume that ESG investors derive a flow of utility from investing in green bonds. Formally, we model this utility flow as a cash-equivalent dividend  $G_t dt$ , per unit of face value. The latter assumption is natural in the ESG context, where the increase in utility investors derive from ESG investing is proportional to the amount invested, and not the current price of the bond.<sup>9</sup> We assume that  $G_t$  also follows an Ornstein-Uhlenbeck process

$$dG_t = \left[ -\mu_g - \phi_g G_t \right] dt + \Sigma_g dW_t^g, \quad (3)$$

where  $W_t^g$  is a Brownian motion uncorrelated with  $W_t^x$ .

We assume that the stochastic discount factor (SDF) is of the linearity-generating (LG)

---

<sup>9</sup>In contrast, Duffie (1996) and D’Amico and Pancost (2021) show that the “dividend” arising from special repo spreads is proportional to the bond’s current price.



form first derived by Gabaix (2007, 2008); it is given by

$$\frac{dM_t}{M_t} = - \left[ \delta_0 + \delta'_1 X_t \right] dt - \left[ \sigma(X_t, G_t) - \begin{pmatrix} \Sigma_x^{-1} X_t \\ \Sigma_g^{-1} G_t \end{pmatrix} X_t' \delta_1 \right] \cdot \begin{pmatrix} dW_t^x \\ dW_t^g \end{pmatrix} \quad (4)$$

where

$$\sigma(X_t, G_t) \equiv \begin{bmatrix} \lambda_0^x + \lambda_1^x X_t \\ \lambda_0^g + \lambda_1^g G_t \end{bmatrix}. \quad (5)$$

Equations (3–5) embed some useful assumptions about the relationship between green spreads and interest rates. First, we assume that  $G_t$  does not affect the drift of the SDF in equation (4); thus, the short rate of interest is independent of  $G_t$ . Moreover, because  $G_t$  does not appear in equation (2) at all,  $G_t$  does not contain any information useful for *forecasting* the short rate, either. Both assumptions allow us to price conventional bonds on a long sample that does not contain any green bonds.

Furthermore, in equation (5) we assume that the time-varying prices of risk  $\sigma(X_t, G_t)$  are “block diagonal” in the sense that the first  $k$  elements depend only on  $X_t$ , while the last element depends only on  $G_t$ . In other words, the price of  $G_t$  risk varies over time only with  $G_t$ ; changes in the nominal yield curve—represented by changes in the first  $k$  factors—have no effect on the price of  $G_t$  risk conditional on the value of  $G_t$ . The converse is also true; the prices of level, slope, and curvature risk can each vary with level, slope, and curvature, but are unaffected by  $G_t$ . These assumptions drastically reduce the number of “green” parameters to estimate, which is particularly important given the short sample for which we observe green bonds.

Although equations (3–5) imply that  $G_t$  and its prices of risk are conditionally independent of  $X_t$ , the model will still allow us to purge the green spreads in equation (1) of most idiosyncratic and confounding factors to recover the greenium. The reason is that the model-implied prices of a green bond will still depend on the conventional factors  $X_t$ , which will be estimated using the full cross-section of German conventional bonds (and not just the green bond’s twin). However, the model might not be able to eliminate completely the impact of  $\tilde{\varepsilon}_t^g$ , to the extent that it is quite different from  $\tilde{\varepsilon}_t$ . This is why in section 5.3, we run corroborating regressions, which allows us to analyze whether indeed the model has done a good job at eliminating the influence of factors unrelated to environmental/climate concerns. An obvious way to eliminate the impact of  $\tilde{\varepsilon}_t^g$  would be to allow  $G_t$  to co-vary with the conventional factors  $X_t$  rather than being independent, but this would drastically increase the number of “green” parameters to estimate, which is not possible given the short

sample for which we observe green bonds. Further, we could try to find a continuous observable proxy of  $G_t$ , but we believe that since we are dealing with environmental preferences and usually preferences are hard to measure, a latent  $G_t$  is more appropriate.

The no-arbitrage pricing condition for a green zero-coupon bond is

$$0 = E_t \left\{ d \left( P_t^g(\tau) M_t \right) + M_t G_t dt \right\}, \quad (6)$$

which, along with the  $X_t' \delta_1$  term in equation (4), ensures that prices of both green and conventional zero-coupon bonds are affine in the state, as the following proposition shows:

**Proposition 1.** *When the state evolves according to equations (2) and (3) and the SDF is given by equation (4), then the price of a conventional security that pays \$1 at time  $T$  when the factors are  $X_t$  is given by*

$$P_t(T - t) = A(T - t) + B(T - t)' X_t, \quad (7)$$

where the functions  $A(\tau)$  and  $B(\tau)$  are given by

$$\begin{pmatrix} A(\tau) \\ B(\tau) \end{pmatrix} = \exp \left\{ - \begin{bmatrix} \delta_0 & \mu_x^{*'} \\ \delta_1 & \phi_x^{*'} + \delta_0 I \end{bmatrix} \tau \right\} \begin{pmatrix} 1 \\ \vec{0} \end{pmatrix}, \quad (8)$$

where  $\exp \{ \cdot \}$  denotes matrix (not element-wise) exponentiation and

$$\begin{aligned} \mu_x^* &\equiv \mu_x - \Sigma_x \lambda_0^x \\ \phi_x^* &\equiv \phi_x - \Sigma_x \lambda_1^x. \end{aligned} \quad (9)$$

On the other hand, the price of a green security that pays a stream of dividends  $G_t dt$  and also pays \$1 at time  $T$  when the factors are  $X_t$  is given by

$$P_t^g(T - t) = A^g(T - t) + B^g(T - t)' X_t + C^g(T - t) G_t, \quad (10)$$

where the functions  $A^g(\tau)$ ,  $B^g(\tau)$ , and  $C^g(\tau)$  are given by

$$\begin{pmatrix} 1 \\ A^g(\tau) \\ B^g(\tau) \\ C^g(\tau) \end{pmatrix} = \exp \left\{ - \begin{bmatrix} 0 & 0 & \vec{0} & 0 \\ \mu_g^* & \delta_0 & \mu_x^{*'} & \mu_g^* \\ \vec{0} & \delta_1 & \phi_x^{*'} + \delta_0 I & \vec{0} \\ \phi_g^* + \delta_0 & 0 & \vec{0} & \phi_g^* + \delta_0 \end{bmatrix} \tau \right\} \begin{pmatrix} 1 \\ 1 \\ \vec{0} \\ 0 \end{pmatrix}, \quad (11)$$

where  $\exp\{\cdot\}$  denotes matrix (not element-wise) exponentiation,  $\mu_x^*$  and  $\phi_x^*$  are defined in equation (9), and

$$\begin{aligned}\mu_g^* &\equiv \mu_g - \Sigma_g \lambda_0^g \\ \phi_g^* &\equiv \phi_g - \Sigma_g \lambda_1^g\end{aligned}\tag{12}$$

*Proof.* See Appendix A.

The linear pricing of Proposition 1 is convenient for pricing coupon bonds, which are portfolios of the zero-coupon bonds priced by equations (7) and (10). In fact, the price of a conventional bond  $i$  at time  $t$  is given by

$$P_{it} = \sum_{j=1}^{n_{it}} c_{ijt} \left[ A(\tau_{ijt}) + B(\tau_{ijt})' \right] \begin{pmatrix} 1 \\ X_t \end{pmatrix}$$

where  $n_{it}$  is the number of total payments for bond  $i$  at time  $t$ ,  $\tau_{ijt}$  and  $c_{ijt}$  are the time and payment amounts of the  $j$ th payment. A similar equation holds for the price of a green bond. Stacking all observable bonds at time  $t$  yields the measurement equation

$$\begin{pmatrix} P_t(\tau_{1,t}) \\ \dots \\ P_t(\tau_{n_t,t}) \\ P_t^g(\hat{\tau}_{1,t}) \\ P_t^g(\hat{\tau}_{2,t}) \\ \dots \end{pmatrix} = \underbrace{\begin{pmatrix} \vec{A}(\tau_{1,t}) & \vec{B}(\tau_{1,t})' & 0 \\ \dots & \dots & \dots \\ \vec{A}(\tau_{n_t,t}) & \vec{B}(\tau_{n_t,t})' & 0 \\ \vec{A}^g(\hat{\tau}_{1,t}) & \vec{B}^g(\hat{\tau}_{1,t})' & \vec{C}^g(\hat{\tau}_{1,t}) \\ \vec{A}^g(\hat{\tau}_{2,t}) & \vec{B}^g(\hat{\tau}_{2,t})' & \vec{C}^g(\hat{\tau}_{2,t}) \\ \dots & \dots & \dots \end{pmatrix}}_{Z(\tau_t, \theta^*)} \begin{pmatrix} 1 \\ X_t \\ G_t \end{pmatrix} + \vec{D}_t \odot \Sigma_t^M \varepsilon_t \tag{13}$$

where  $\vec{A}$ ,  $\vec{B}$ ,  $\vec{A}^g$ ,  $\vec{B}^g$ , and  $\vec{C}^g$  are coupon-weighted sums of the relevant bond-price loadings,  $\tau_{i,t}$  is the vector of payments and times to maturity of bond  $i$ 's payments at time  $t$ , and  $\Sigma_t^M$  is the variance of the measurement error at  $t$ . Pricing dozens of bonds with only a few factors requires the assumption that all prices are observed with some error. The vector  $\vec{D}_t$  contains the duration of each bond, which scales the measurement error in prices; doing so essentially weights each price observation by its inverse duration, akin to assuming that the measurement error is homoskedastic (to a first-order approximation) in yields rather than prices (Pancost, 2021). Omitting the  $\vec{D}_t$  term from equation (13) would result in a model fitting the long end of the yield curve much better than the short end.

Importantly, the elements of the vector  $\varepsilon_t$  are a combination of  $\tilde{\varepsilon}_{i,t}$ ,  $\tilde{\varepsilon}_{i,t}^g$ ,  $\tilde{\varepsilon}_t$ , and  $\tilde{\varepsilon}_t^g$  from

equation (1).

To estimate the model, in practice it is convenient to focus on the risk-neutral parameters  $\theta^* \equiv \{\delta_0, \delta_1, \mu_x^*, \phi_x^*, \mu_g^*, \phi_g^*\}$ , rather than the prices of risk  $\{\lambda_0^x, \lambda_1^x, \lambda_0^g, \lambda_1^g\}$ . The reason is that the matrix  $Z(\tau_t, \theta^*)$  does not depend on the latent factors  $X_t$  and  $G_t$ —it depends only on the data (through  $\tau_t$ ) and  $\theta^*$ . Independence from the factors means that  $Z(\tau_t, \theta^*)$  can be constructed from the data and risk-neutral parameters alone, and then the factors can be estimated cross-section by cross-section using ordinary least squares and the sequential regression filter of [Andreasen and Christensen \(2015\)](#). This estimation approach—when combined with the LG model—is an order of magnitude faster than can be achieved using a standard exponential-affine model, where the time-series parameter  $\Sigma_x$  also appears in the measurement equation ([Pancost, 2021](#)).

Because the factors  $X_t$  and  $G_t$  are unobservable, not all of the parameters in  $\theta^*$  are identifiable. In particular, since any affine transformation of the  $X_t$  leads to the same fit to bond prices, only the eigenvalues of the matrix in equation (8) are identified. Thus, rather than estimating all  $(k+1)^2$  free parameters in this matrix, we normalize  $\delta_1 = \begin{bmatrix} 1 & \vec{0} \end{bmatrix}'$  and  $\phi_x^{*'} + \delta_0 = I$ .<sup>10</sup> In the end, only the  $k+1$  parameters in  $\delta_0$  and  $\mu^*$  need to be estimated, when pricing conventional bonds. Pricing green bonds implies an additional two risk-neutral parameters, as can be seen in equation (11).

Given an estimate of  $\theta^*$ , we estimate a latent vector of conventional factors  $X_t$  and the latent green factor  $G_t$  on each date; we do so using the sequential regression filter of [Andreasen and Christensen \(2015\)](#), which also allows us to estimate the time-series parameters in equations (2) and (3). We estimate the parameters pertaining to  $X_t$  on a long sample of conventional bond prices from October 27, 2008 to August 30, 2022. Because the model effectively de-couples the time-series and price-of-risk parameters for  $X_t$  and  $G_t$ , the time-series variation is relevant only to estimate expected returns, so that the benchmark greenium is identified solely from the cross-section of bond prices. Appendix B contains more details about our estimation procedure and estimated parameter values.

## 4 Results

In this section we discuss the results of estimating the model on conventional and green German sovereign securities. Section 4.1 describes the model’s fit to the data, Section 4.2 describes our estimated German greenium, and Section 5 uses the model to estimate expected returns on green and conventional bonds and compares them with the greenium.

---

<sup>10</sup>This normalization, though more complicated than (for example)  $\mu^* = \vec{0}$  and a diagonal  $\phi_x^*$ , does not restrict the estimated eigenvalues to be real—and in fact four of the five estimated eigenvalues are complex.

## 4.1 Model Fit

Although the standard practice in the fixed-income literature is to estimate sovereign nominal bond yields using three latent factors (Litterman and Scheinkman, 1991; Cochrane and Piazzesi, 2008), because we use maturities out to thirty years, we need four latent factors. The conventional wisdom that three factors are sufficient applies only to bonds with a maximum of 10 years left to maturity, which is the main focus of the vast majority of the DTSM literature, with a few exceptions (Berardi, Brown and Schaefer, 2021). But, one of the four German green bonds has 30 years to maturity, and we certainly do not want to lose this observation. Pricing these very long-maturity bonds requires an additional factor, especially later in the sample when the 1–10 year yield-curve slope is steep, but the 10–30 slope is relatively flat (see the bottom panel of Figure 5).

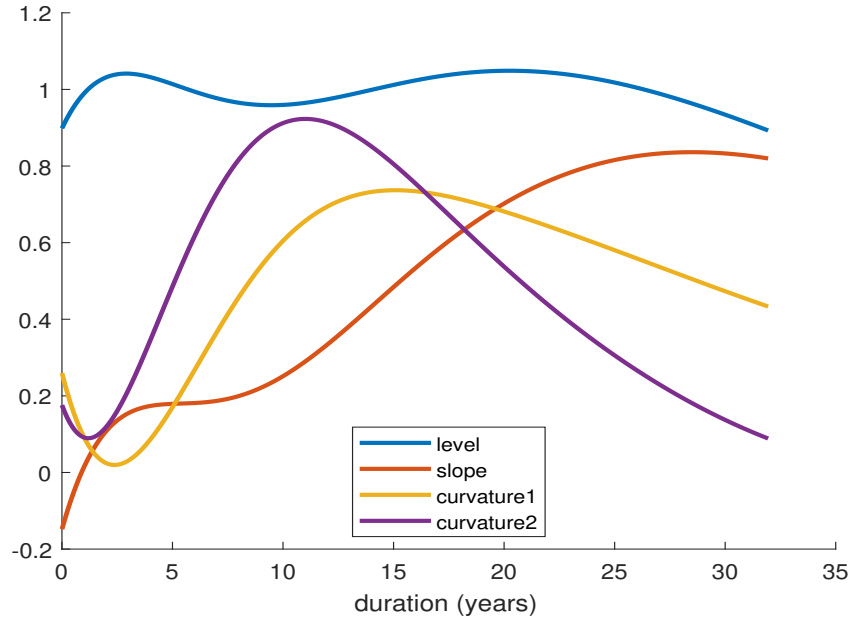


**Figure 6.** Conventional Bond Factor Loadings

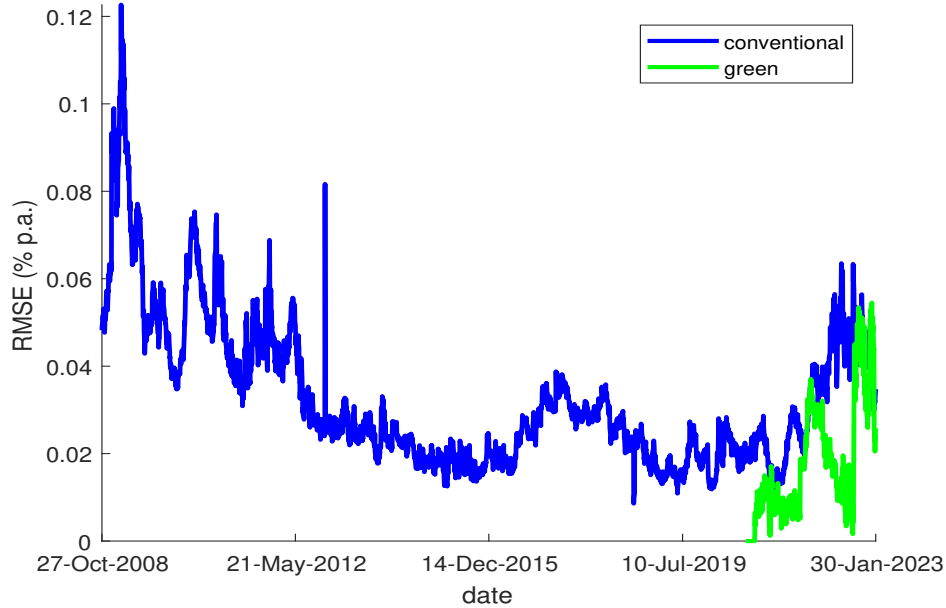
The figure plots the yield factor loadings  $B^y(\tau)$  as a function of maturity  $\tau$  at the average value of the factor  $\bar{X}$ .

Figure 6 plots the conventional yield loadings of the estimated linearity-generating (LG) model described in the previous section, which, being a 4-factor model of conventional bonds, includes two curvature factors rather than one. Differently from the standard exponential-affine models, those loadings represent the first derivative of the log yield at maturity  $\tau$ ,

which is given by

$$B^y(\tau, X) \equiv \frac{\partial}{\partial X} \left\{ -\frac{1}{\tau} \log P_t(\tau) \right\} \\ = \frac{-B(\tau)}{\tau [A(\tau) + B(\tau)' X]}.$$

The loadings in Figure 6 are evaluated at the sample average of the factors  $X_t$ .



**Figure 7.** Fit to Conventional Bonds

The figure plots the model root mean squared error (RMSE) in annualized percent over time for model of Proposition 1 estimated on a panel of German sovereign bonds, omitting the four green bonds.

Figure 7 plots the model fit to conventional securities over time in terms of root mean squared error (RMSE). Not surprisingly, as in all DTSMs, the model fit is poorest in late 2008, during the tail end of the financial crisis. The model fit then improves gradually over time, with the RMSE falling to between 1–2 bps by 2015. In recent months it has begun to increase again, to 5–6 bps. Notice that apart from late 2008, the model’s RMSE is roughly the same order of magnitude as the green spreads plotted in Figure 4. In this sense, the model may have trouble picking out any greenium at all: the (small!) differences between green and conventional twin yields are on average not much bigger than the yield differences between any two conventional bonds with similar duration. However, this is not the case: in fact, apart from the first weeks of the sample, the model will imply a greenium that is often

larger than the green spreads in Figure 4.

Table 2 reports the model fit for bonds of various maturities and for subsets of the securities. The top panel reports the average price residual, while the bottom panel reports the RMSE. In particular, the top row in each panel reports average price residual and RMSE for the model estimated on the full sample of conventional bonds. The other rows report results from models with the same risk-neutral parameters  $\theta^*$ , but estimated only on data after the issuance of the first German green bond (September 9, 2020). The rows labeled “All Data” estimated the factors  $X_t$  using all available bond prices, while the rows labeled “Twins Only” and “Greens Only” overweight the conventional twins and green bonds, respectively. This is done by prioritizing either the 4 conventional twins only, or the 4 green bonds only, which implies that the model is forced to fit them exactly sacrificing other securities. In each experiment, this is somewhat equivalent to assume that the 4 securities of interest are observed without errors.

Average price residuals for the full-sample and all-bond estimations in Table 2 are close to zero, as they should be. On the other hand, the “Twins Only” and “Greens Only” models have average price residuals of about +6 bps and +3 bps, respectively, across all maturities, mainly driven by extreme overpricing of securities in the 2–3 year range. Price residuals in the “Greens Only” model for bonds between 4–10 years are negative, reflecting the facts that (i) 3 of the 4 green bonds are in this maturity range, and (ii) the green bonds do have slightly higher prices on average than conventional bonds with similar maturity. In contrast, price residuals at the short end of the curve with less than three years to maturity are on the order of +10–25 bps.

In other words, the “twin” bonds are not representative of the entire German yield curve. A model focusing only on twin yields in the medium-to-long end of the maturity range leads to biased estimates of bond prices at *all* maturities, by over-pricing short-maturity bonds and under-pricing longer-maturity bonds. Because there are many more shorter-term securities, and the bias is larger there, the overall bias is positive.

Focusing exclusively on “twin” bonds not only induces bias, it also leads to noisier estimates. Panel B of Table 2 reports the RMSE for models estimated on the full sample, the green sample, and the green and twin bonds, respectively. RMSEs for models estimated on all bonds are between 2–4 bps, at all maturities and for both the full and post-2020 samples. However, the overall RMSE when focusing only on twin or green bonds is much higher, at 16.7 and 20.5 bps respectively. Similar to the average price residuals in Panel A, most of the poor fit comes from the short end of the yield curve, where the RMSE is between 18–44 bps. This is due to the fact that there are not yet conventional twins and green bonds with less than 3 years left to maturity. The RMSE for bonds greater than 15 years is also quite

high at about 8–9 bps. By ignoring most of the data, models fit to the twin and green bonds only do a poor job of pricing the full cross-section of German bonds.

Model	Maturity Range							
	All	< 2	[2, 3)	[3, 4)	[4, 5)	[5, 10)	[10, 15)	$\geq 15$
Panel A: Average Residual								
Full Sample from Sept 2020	0.0005	-0.00235	0.00852	0.0052	-0.00803	0.00348	-0.00987	-0.000822
All Bonds	-0.000443	0.00687	-0.0109	-0.00804	-0.013	0.00826	-0.0344	0.00426
Twins Only	0.0587	0.258	0.119	0.022	-0.0219	-0.00438	0.0262	0.0192
Greens Only	0.0277	0.251	0.101	-0.0135	-0.064	-0.0553	-0.00337	0.00469
Panel B: RMSE								
Full Sample from Sept 2020	0.0342	0.0271	0.0307	0.0297	0.0276	0.0366	0.0398	0.041
All Bonds	0.0332	0.0368	0.0317	0.0218	0.0233	0.0311	0.0539	0.0335
Twins Only	0.167	0.362	0.183	0.0448	0.0437	0.0499	0.0828	0.082
Greens Only	0.205	0.438	0.217	0.0447	0.0893	0.0861	0.103	0.0896

**Table 2.** Model Fit

The table reports average residual (panel A) and root mean squared error (panel B) in annualized percent for various models and for bonds of different maturities. The residuals are defined as actual minus model-implied price, scaled by duration, and are thus in units of annualized percent. The first column reports the overall statistic; subsequent columns report statistics for bonds with less than 2, between 2–3, 3–4, 4–5, 5–10, 10–15, and greater than 15 years remaining maturity, respectively. The first row of each panel reports results for the full sample; subsequent rows report results for the sample restricted to post September 8, 2020 (i.e., when the first green bond appears in the data). The row labeled “All Bonds” uses all bonds on this sub-sample; the row labeled “Twins Only” reports results in which the factors  $X_t$  are estimated to closely match the prices of the conventional twin bonds, while the last row in each panel reports results in which the factors  $X_t$  are estimated to closely match the prices of the green bonds.

If we were to focus only on the 4 pairs of green securities and their twins, we would extract less accurate conventional and green yield curves, and therefore less accurate fundamental pricing factors as well as the green factor. This is because the prices of these 4 pairs of securities do not contain enough information about the front end of the yield curve, which is mostly determined by the stance of monetary policy, and also would not provide accurate information about the slope of the yield curve, which is a strong predictor of recessions. This, in turn, implies that focusing only on the 4 green spreads does not properly control for the fundamental factors driving both green and conventional securities, which results in



a less precise identification of the green factor and associated greenium.

## 4.2 Estimated Greenium

The blue line in Figure 8 plots the model’s estimate of the German 10-year greenium; that is, the yield difference between a 10-year constant maturity green bond and a 10-year constant-maturity conventional bond. First of all, it is evident that the fundamental greenium varies significantly over time, a feature that is unveiled because of the use of a dynamic pricing model. This, in turn, will allow us to study the economic and financial drivers of the greenium over time.

Specifically, the model-implied greenium averages to about 4 basis points over the sample period (3.5% of the average 10-year yield in the sample). In the first few months, it is close to zero; this is driven by the fact that the conventional twin bonds at this time are in fact over-priced, according to the model, by an amount equal to the green spread. Then it increases significantly in the summer of 2021, most likely as investors’ attention to climate change is heightened by the devastating German floods. Finally, it widens sharply in the last week of February 2022 following a shock to energy prices due to the Ukraine invasion, and it continues to widen reaching a peak of about 7 basis points in the summer of 2022.

Figure 8 also plots the greenium at the 5- and 30-year maturities. To help build intuition for the term structure of the greenium, Figure 5 plots the German yield curve on two dates, July 15 2021 and April 19, 2022. The former date is an example of a cross-section of yields in which the model does reasonably well, with an RMSE of 1–2 bps. The model-implied zero-coupon yield curve (red line) is reasonably close to the actual yields, though the fit is much better at the short end of the yield curve where there are more bonds.<sup>11</sup> In contrast, mid-April 2022 presents a challenge for any term structure model to price, because the yield curve is extremely steep from 1–10 years duration and then close to flat afterwards. This is also the reason why the 4-factor model performs better than the 3-factor model for conventional securities. In both cases, the model-implied greenium at any maturity is the difference between the red and green dashed lines.

---

<sup>11</sup>Note that the model is *not* estimated to minimize the squared residuals between the red line and the black dots; the latter, being yields to maturity on coupon-paying bonds, might diverge from the zero-coupon curve.

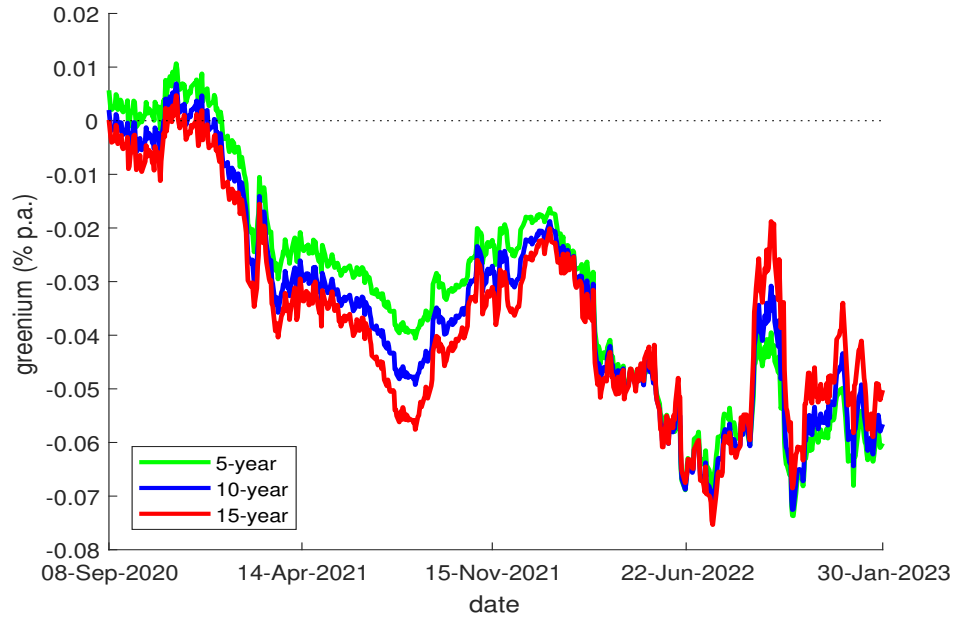


**Figure 8.** German Greenium at Various Maturities

The figure plots the German greenium in annualized percent over time, defined as the yield difference between a zero-coupon green bond and a zero-coupon conventional bond with the same maturity. The green line plots the 5-year greenium, the blue line plots the 10-year greenium, and the red line plots the 30-year greenium.

While Figure 5 can be used to infer the term structure of the greenium on one date, Figure 8 also reports the term structure of the greenium over time by plotting the model-implied 5-, 10-, and 30-year greeniums. It is upward-sloping: the 30-year greenium is always larger than the 5-year greenium. Further, the slope of term structure does not appear to be constant over time. It is quite flat at the beginning and end of the sample, while it is steep in the second half of 2021, when the 30-year greenium reaches its peak of 8 basis points and the 5- and 10-year greenium hover around 4 basis points. Following the start of the war in Ukraine and related spike in energy prices, all the greeniums start moving closely together, with the shorter maturities widening as much as the 30-year.

This stays in sharp contrast with the downward-sloping term structure of the green spreads, displayed in Figure 4, where starting in September 2021 the 5-year green spread is always larger than the 30-year spread. Actually, by the end of the sample period, the 10- and 30-year green spreads almost revert to zero, suggesting that, despite the German floods and the spikes in energy prices, at these horizons environmental concerns have improved rather than worsening. Unless, factors other than environmental preferences have dominated the fluctuations of the green spreads but not those of the model-implied greeniums at similar maturities.

### 4.3 The Drivers of the Greenium

In this section, we contrast our estimated 10-year constant-maturity greenium with the green spread on the first German pair of twin bonds which has a similar maturity, both plotted in Figure 9. Although there is a spread between the two measures, they roughly track each other for the first half of the sample, including in late 2021 when they both widen. However, after the start of the war in Ukraine in February 2022, the green spread narrows while the greenium widens. This occurs at roughly the same time that the German stock market begins to perform poorly, just as oil and gas prices begin to skyrocket.

To formally analyze what drives a wedge between these two measures, we relate them with various proxies of shocks to environmental preferences, and confounding/idiosyncratic factors unrelated to such preferences. We find that the green spread is correlated with the confounding/idiosyncratic factors while the greenium is not. Furthermore, the greenium is significantly related with proxies of shocks to environmental/climate concerns, but the green spread is not, or is correlated with the wrong sign. This leads us to conclude that our model does seem to “purge” green spreads of most factors unrelated to investor’s environmental preferences, lending credence to the notion that we have uncovered the fundamental component of the greenium.

To proxy for shocks to investors’ preferences for green securities, we use oil futures prices and a measure of the damages directly caused by all major natural disasters in Europe (in billions of U.S. dollars).<sup>12</sup> The first measure mostly captures the sharp increase in energy prices following the Ukraine invasion in February 2022, which particularly affected Germany, and may have further stressed the need to reduce the dependence on fossil fuel and accelerate the transition toward clean energy.<sup>13</sup> The second measure of shocks to climate concerns is mainly driven by the floods that disrupted Germany in July 2021.

To proxy for confounding/idiosyncratic factors that might drive the wedge between the greenium and the green spread as unrelated to climate concerns, we looked for indicators that capture purely financial motives (such as flight-to-quality) as well as those related to demand and supply imbalances between conventional and green bonds. For the former, we use the German stock-market price index (DAX) and the implied volatility index (VIX). To capture demand imbalances, we exploit the relative differences in the stock and flow of assets in the top 20 Eurozone-focused fixed-income government-style ESG and non-ESG funds. Specifically, we use three proxies for demand imbalances: the number of new ESG funds

---

<sup>12</sup>We obtain the data from the [International Disaster Database EM-DAT](#), which is freely available. The data also includes an estimate of the death toll from each disaster; although this variable lacks the coverage of the economic damages, our results are similar if we use it, instead.

<sup>13</sup>We have also used gas prices and obtained the same results not shown for brevity.

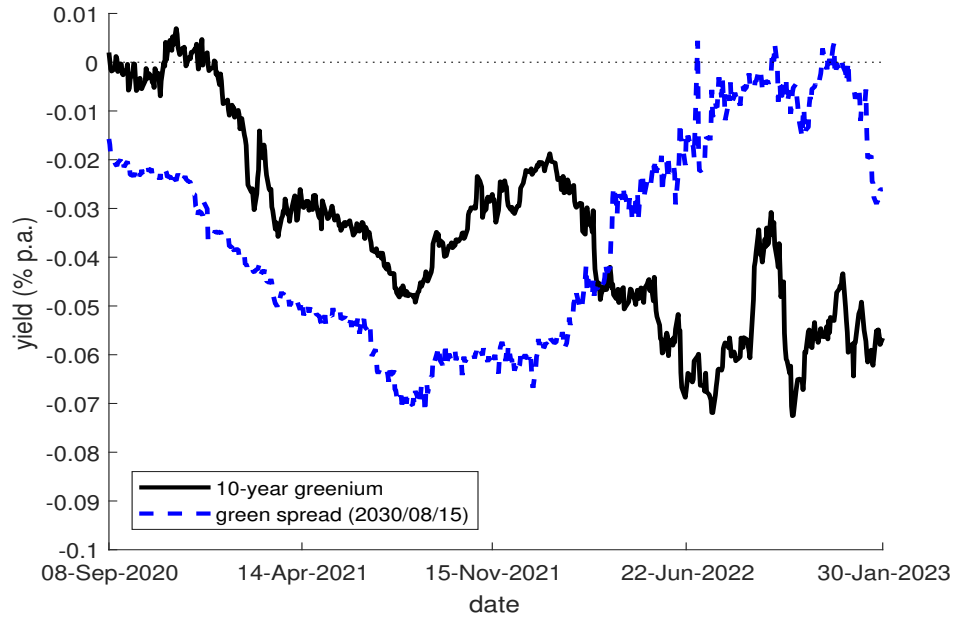


**Figure 9.** 10-Year Greenium and 2030/08/15 Green Spread

The figure plots the model-implied 10-year greenium from Figure 8 (black line) against the green spread for the first pair German green and conventional bonds from Figure 4 (blue dotted line). Both measures are plotted in annualized percent.

opening each week, the difference in the weekly growth rates of assets under management (AUM) at ESG and non-ESG funds, and the difference in the weekly net flows into ESG and non-ESG funds as percentage of total AUM. To capture supply imbalances, we use dummy variables for the dates of the re-openings of the green and conventional twin bonds.

All of these proxies of flight-to-quality and relative scarcity may also be capturing temporary liquidity differentials between conventional and green bonds—which are also factors unrelated to environmental preferences.

Finally, we also include a dummy that equals one on the week (July 4, 2022) in which the ECB announced major steps to expand its climate-related framework. All the measures announced on that day might have been perceived as significantly increasing the probability of the ECB shifting its balance sheet, facilities, and unconventional monetary policy toward greener assets, increasing their value. This, in turn, should translate into a larger greenium because of the ECB’s regulatory support for green assets. This type of greenium, which we label “regulatory” greenium, could derive from the interaction of environmental preferences with the fundamentals of the economy, in this case the stance of monetary policy. In other words, it could derive from the interaction of  $X_t$  and  $G_t$ , which our model does not take into account.

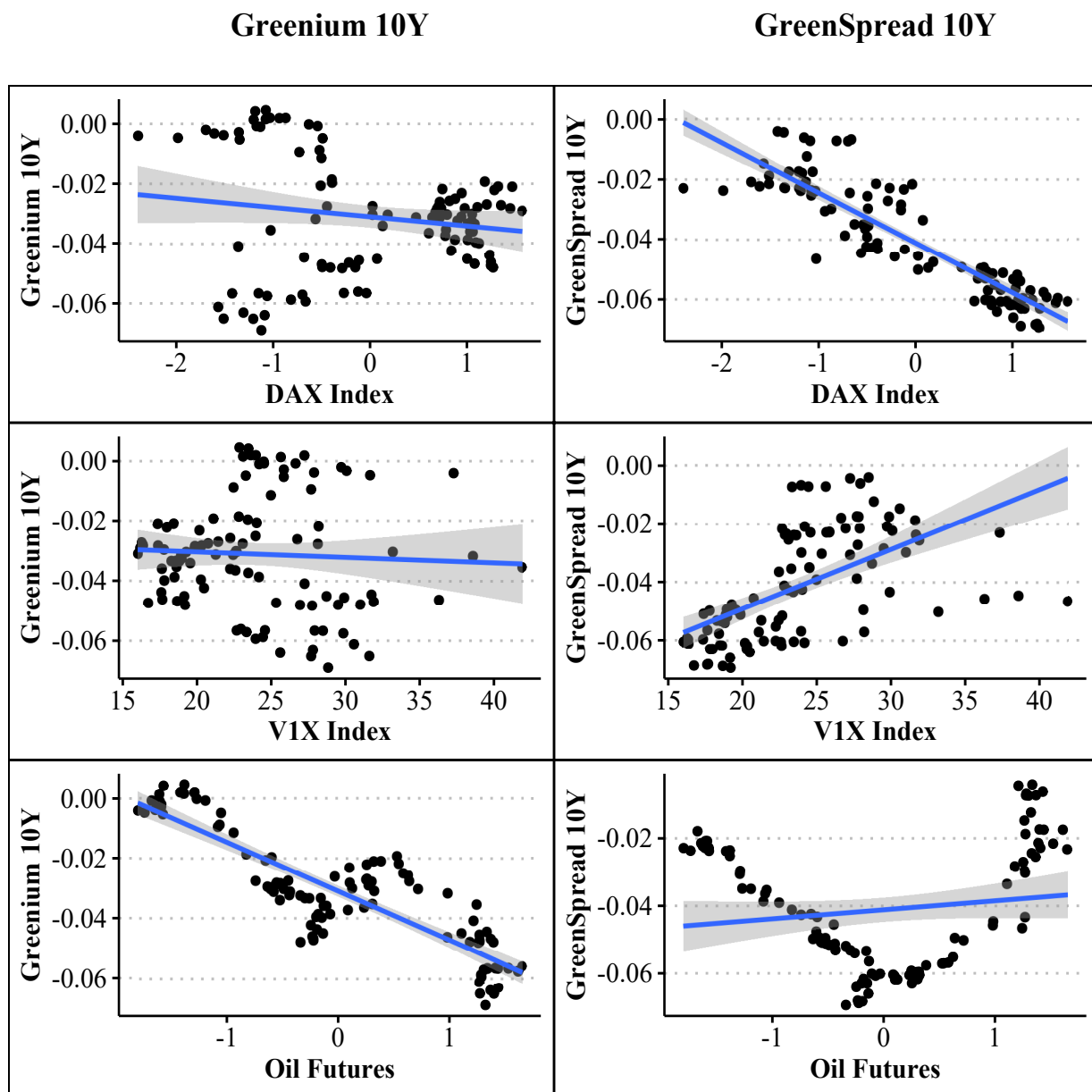


**Figure 10.** Regression Scatterplots

The figure plots scatter plots of the 10-year model-implied greenium (left column) and the green spread between the oldest German green bond and its conventional twin (right column) against the German DAX index, the V1X index, and the EU Brent Crude Oil Forward (first, second, and third rows, respectively). The blue lines report the coefficient estimates with 95% confidence intervals marked in gray of the univariate regressions.

Figure 10 visualizes the univariate relation between the 10-year model-implied greenium and the green spread with three key proxies: the German stock-market price index (DAX), the German stock-market implied volatility (V1X), and the EU oil future prices. While the

green spread is strongly negatively correlated with stock-market prices and positively correlated with stock-market volatility, the model-implied greenium is barely affected by these two variables, suggesting that it is not driven by financial motives. For instance, flight-to-quality episodes in which stock prices decline and the V1X spikes seem to be associated with a shrinking green spread, as investors favor the more liquid conventional bonds relative to the green bonds. Such episodes are unrelated to environmental preferences, and indeed the greenium reacts quite differently. In contrast, the model-implied greenium is strongly negatively related to future oil prices, one of our proxies for shifts in environmental preferences, while the green spread is hardly affected by it.

To better quantify the relationship between the greenium and all of the proxies described above, and verify whether the model has indeed purified the greenium from idiosyncratic and confounding risk factors unrelated to environmental preferences, we run the following regressions:

$$y_t = \beta_0 + \beta_1 \text{DAX}_t(\text{or V1X}_t) + \beta_2 \text{Oil Fut}_t + \beta_3 \text{NatDisast}_t \\ + \beta_4 \text{DemandImb}_t + \beta_5 \mathbb{1}(\text{Reop}) + \beta_6 \mathbb{1}(\text{ECB}) + \varepsilon_t, \quad (14)$$

where  $y_t$  is either our model-implied 10-year greenium, or the green spread on the oldest German green bond maturing on August 15 2030, or the fitting errors relative to the green yield curve. The last dependent variable, should help illustrate that the idiosyncratic and confounding factors affecting the green spread are indeed ending up in the model residuals.

Table 3 shows that, while the model-implied greenium is mostly affected by proxies of shocks to environmental/climate concerns, the green spread is strongly affected by the different proxies of idiosyncratic and confounding factors, such as the stock-market prices and some of the measures of relative scarcity. Our estimates imply that a one-billion increase in damages from natural disasters causes the greenium to increase by about 0.04 basis points, indicating that the natural disasters alone explain about 1.6 basis points of the greenium’s average size magnitude. On the other hand, the green spread does not seem to be statistically-significantly related to natural disaster damages. Moreover, its coefficient on the other proxy of climate concerns (future oil prices) has the wrong sign, which seems to be driven by the residual term (columns 3 and 6). At the same time, the proxies for demand/supply imbalances never matter for the greenium, though they sometimes correlate with the green spread. Interestingly, the ECB announcement about its climate-related framework is significant for the greenium, indicating that the model has not purged the “regulatory” component of the greenium as, most likely, it derives from the interaction of  $G_t$  and  $X_t$ . Jointly, the proxies of shift in environmental/climate concerns and the ECB

announcement explain 75% of the variation in the model-implied greenium.

	<i>Dependent variable:</i>					
	GreenSpread	Greenium	Residual	GreenSpread	Greenium	Residual
	(1)	(2)	(3)	(4)	(5)	(6)
DAX Index	−2.23*** (0.12)	−0.24 (0.17)	−0.72 (1.08)	−2.38*** (0.105)	−0.15 (0.14)	−2.52*** (0.72)
Oil Futures	0.81*** (0.16)	−1.55*** (0.22)	5.04*** (1.08)	0.46*** (0.063)	−1.36*** (0.088)	1.44*** (0.36)
Natural Disasters	−0.06 (0.06)	−0.22** (0.09)	−0.72 (0.36)	−0.08 (0.07)	−0.21** (0.09)	−0.72 (0.36)
N. ESG Funds	−0.06** (0.025)	0.03 (0.035)	−0.72*** (0.36)			
Net Fund Flows				6.65 (8.69)	2.85 (11.98)	89.28 (68.04)
Reopening Green	−0.72 (0.49)	−0.31 (0.69)	1.44 (3.96)	−0.87* (0.51)	−0.28 (0.70)	1.08 (3.96)
Reopening Conv.	0.69* (0.41)	0.36 (0.58)	−0.36 (3.24)	0.73* (0.42)	0.36 (0.59)	−0.72 (3.24)
ECB An. 7/4/22	−0.72 (0.51)	−1.50** (0.71)	−1.44 (3.96)	−0.87* (0.52)	−1.39* (0.71)	3.96 (3.96)
Observations	104	104	104	104	104	104
Adjusted R <sup>2</sup>	0.868	0.758	0.211	0.861	0.756	0.147

**Table 3.** Drivers of the Greenium and Green Spread (DAX)

The table reports the results of estimating equation (14) on weekly data from September 8, 2020 to August 30, 2020, including the DAX as an independent variable. “Natural Disasters” refers to the total economic damages, in billions of U.S. dollars, from all major natural disaster in Europe (from the [International Disaster Database EM-DAT](#)). “N. ESG Funds” is the number of new ESG funds opening each week. “Net Fund Flows” is the difference in the weekly net flows into ESG and non-ESG funds as percentage of total AUM. “Reopening Green” and “Reopening Conv.” are indicator variables for weeks in which the GFA reopened the green bond or its conventional twin, respectively. “ECB An. 7/4/22” is an indicator for the week of July 4, 2022, when the ECB announced major steps to expand its climate-related framework. \*p<0.1; \*\*p<0.05; \*\*\*p<0.01

Table 4 repeats the exercise using the V1X in place of the DAX. The results are broadly similar, although in this case the greenium does seem to correlate somewhat with the V1X (though not as strongly as the green spread). This result is due to the interaction of V1X with the other regressors, because we have already shown in the univariate regressions plotted

in Figure 10 that VIX has not significant relation with the greenium and actually its slope coefficient is slightly negative rather than positive. However, the  $R^2$ s in columns 1 and 4 of Table 3 are much higher than the same columns in Table 4, suggesting that the stock market explains more of the deviation between greenium and green spread than the volatility index.

	<i>Dependent variable:</i>					
	GreenSpread	Greenium	Residual	GreenSpread	Greenium	Residual
	(1)	(2)	(3)	(4)	(5)	(6)
VIX Index	1.13*** (0.25)	0.58*** (0.17)	2.16** (1.08)	1.57*** (0.27)	0.50*** (0.16)	3.60*** (1.08)
Oil Futures	1.67*** (0.30)	-1.67*** (0.21)	4.68*** (1.08)	0.105 (0.14)	-1.42*** (0.085)	1.08** (0.36)
Natural Disasters	-0.12 (0.13)	-0.20** (0.09)	-0.36 (0.36)	-0.24 (0.15)	-0.18** (0.09)	-0.72 (0.36)
N. ESG Funds	-0.24*** (0.042)	0.04 (0.03)	-0.72*** (0.036)			
Net Fund Flows				22.83 (18.72)	-0.37 (11.47)	-91.08 (66.60)
Reopening Green	-0.19 (0.95)	-0.71 (0.67)	-0.036 (3.96)	-0.74 (1.11)	-0.65 (0.68)	-0.36 (3.96)
Reopening Conv.	1.60** (0.79)	0.42 (0.55)	-0.36 (3.24)	2.11** (0.90)	0.35 (0.55)	0.36 (3.24)
ECB An. 7/4/22	1.31 (0.94)	-1.59** (0.66)	-2.16 (3.60)	1.18 (1.09)	-1.55** (0.67)	-2.88 (3.96)
Observations	104	104	104	104	104	104
Adjusted R <sup>2</sup>	0.547	0.78	0.245	0.395	0.77	0.175

**Table 4.** Drivers of the Greenium and Green Spread (VIX)

The table reports the results of estimating equation (14) on weekly data from September 8, 2020 to August 30, 2020, including the VIX as an independent variable. “Natural Disasters” refers to the total economic damages, in billions of U.S. dollars, from all major natural disaster in Europe (from the [International Disaster Database EM-DAT](#)). “N. ESG Funds” is the number of new ESG funds opening each week. “Net Fund Flows” is the difference in the weekly net flows into ESG and non-ESG funds as percentage of total AUM. “Reopening Green” and “Reopening Conv.” are indicator variables for weeks in which the GFA reopened the green bond or its conventional twin, respectively. “ECB An. 7/4/22” is an indicator for the week of July 4, 2022, when the ECB announced major steps to expand its climate-related framework. \*p<0.1; \*\*p<0.05; \*\*\*p<0.01



## 5 Expected Returns

While the greenium—defined as a difference in yields, and thus a difference in discount rates applied to green and conventional bonds—is an object of interest in its own right, the model also allows us to estimate differences in *expected returns* between green and conventional bonds, that is, the expected green excess returns. Both the green and conventional twin bonds have negative yields in most of our sample, implying that the expected returns from holding either of them to maturity are negative. Moreover, because the green bonds have lower yields than their twins (Figure 4), the green bonds have an even lower expected return. However, yields are only expected returns from holding bonds to maturity;<sup>14</sup> it is possible for expected returns from shorter holding periods to diverge from yields, especially for longer-maturity bonds.

A key advantage of estimating a DTSM is that it allows us to compare the realized returns with expected returns of the same holding period. Figure 11 plots realized (in black) vs. expected (in red) returns for each of the four portfolios that go long the German green bond and short the corresponding conventional twin. What differs across the four panels is the maturity of the underlying bonds.

The expectation, which is derived from the estimated DTSM by iterating equations (2) and (3) forward in time, is taken on the first day of trading for each bond; that is, the figure plots

$$\begin{aligned} & 100 \times \left[ E_t \left\{ P_{i,t+h}^g - P_{i,t+h} + \varepsilon_{i,t+h}^g - \varepsilon_{i,t+h} \right\} - \left( P_{i,t}^g - P_{i,t} \right) \right] \\ & = 100 \times \left[ E_t \left\{ P_{i,t+h}^g - P_{i,t+h} \right\} + \rho^h \left( \varepsilon_{i,t}^g - \varepsilon_{i,t} \right) - \left( P_{i,t}^g - P_{i,t} \right) \right] \end{aligned} \quad (15)$$

where  $t+h$  runs along the  $x$ -axis,  $t$  is fixed at the first trading date of each bond, and  $P_{i,t+h}^g$  and  $P_{i,t+h}$  are the prices of the German green bond and its conventional twin, respectively, at  $t+h$ .<sup>15</sup> We use the subscript  $i$  in equation (15) because for this exercise we consider the actual twin bonds, whose maturity changes deterministically over time, rather than a synthetic constant-maturity pair as in for example Figure 8.

<sup>14</sup>Strictly speaking, this statement is only true for zero-coupon bonds—as all the German green and conventional twin bonds happen to be. Once a bond pays coupons, its yield to maturity and expected return to maturity will differ, since the coupon payments must be reinvested at unknown future yields. This difference between expected returns and yields to maturity will be all the more important going forward, as rising interest rates imply that German bonds will no longer be zero-coupon. Indeed, the fifth German green bond (issued on September 7, 2022) pays a 1.3% coupon.

<sup>15</sup>Because the model does not price either bond perfectly at  $t$ , but the expectations of future prices do not contain any measurement error, the second term in equation (15) represents a forecast of future bond-level measurement errors. The parameter  $\rho \approx 0.99$  is the estimated autocorrelation of the bond-level pricing residuals from equation (13).

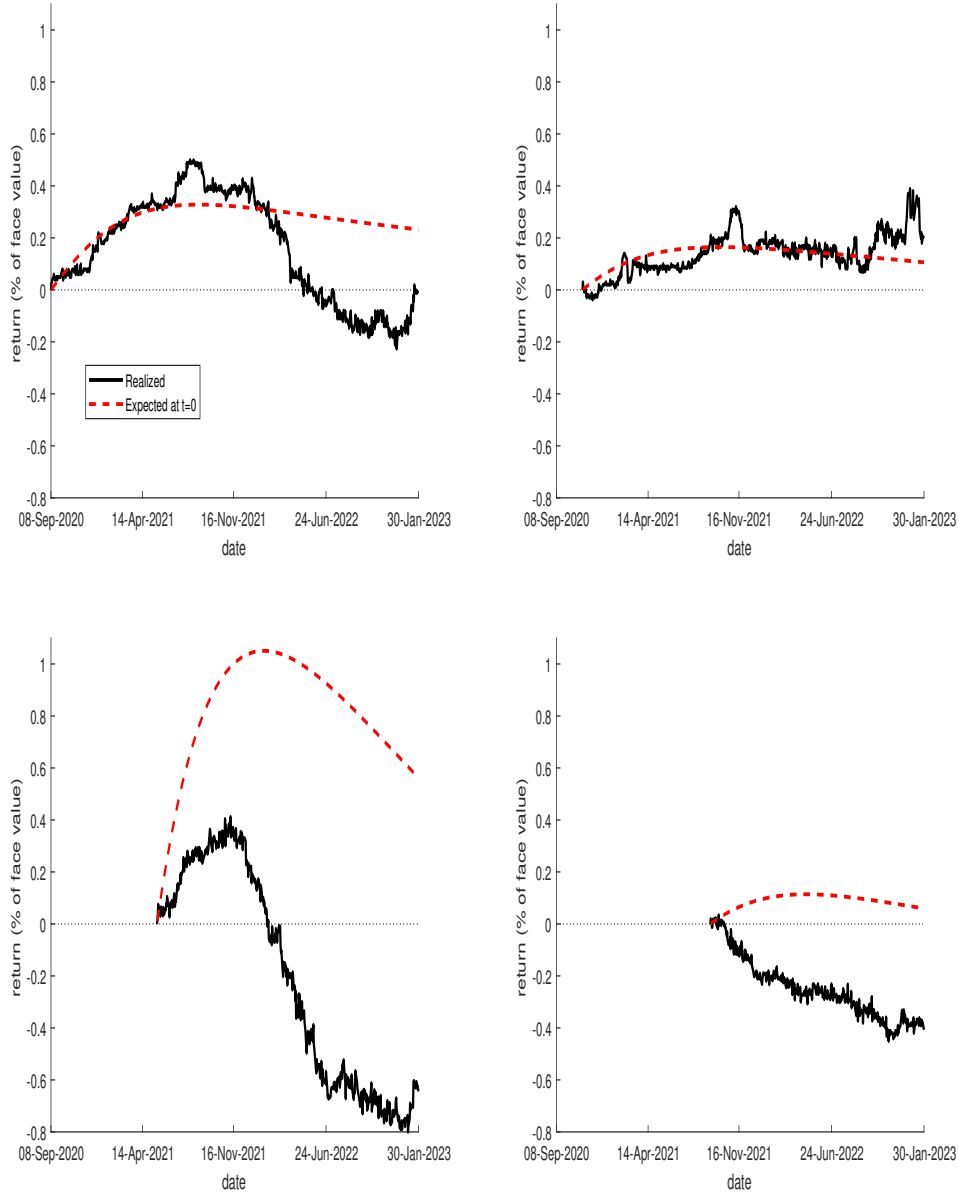


**Figure 11.** Realized and Expected Excess Returns on German Twins

The four panels plot the realized cumulative excess returns on the four German twin pairs over time, according to equation (15), where  $t$  is fixed and  $t + h$  runs along the  $x$ -axis. The solid black line plots the realized return, while the dashed red line plots the expected return at  $t$ .

Figure 11 shows that, for the three pairs of twins issued before the German floods (top panels and bottom left panel), the expected green excess returns are positive. Because our model is dynamic, rather than static as in Pastor, Stambaugh and Taylor (2021), it can generate positive expected green excess returns in some periods, in particular when the greenium is above its sample mean (as it is close to zero, rather than negative, at the start

of the sample). In this case, mean reversion of the greenium implies that green bonds will *temporarily* appreciate relative to their conventional twins, leading to a positive expected green excess return over a short investment window.<sup>16</sup> The size and expected path of this positive excess return depends on the estimated speed of mean reversion of  $G_t$ —i.e. the parameter  $\phi_g$ —which is difficult to estimate on a short sample period. However, the sign of the expected green excess return is unaffected by  $\phi_g$  (so long as  $G_t$  is stationary).

In contrast, for the pair of twins issued soon after the German floods (bottom right panel of Figure 11), the expected green excess returns are practically zero. This seems to suggest that, once climate concerns increase because of the devastating consequences of the German floods, investors are willing to accept lower expected returns on green bonds to subsidize the government’s green projects.<sup>17</sup> This is also consistent with the widening green spread and greenium immediately after the German floods of July 2021.

Further, in the top two panels of Figure 11, realized and expected green excess returns are quite close to each other. However, in early May 2021, as Germany’s federal cabinet unexpectedly sets tougher CO2 emission reduction targets after the surprising top court rulings,<sup>18</sup> green bonds start performing better than expected. The gap between realized and expected green excess returns increases further following the German floods in July 2021. In other words, as the German government signals a stronger commitment to reduce the impact of climate change and investors become more concerned about its consequences, the prices of green bonds increase relative to conventional bonds, most likely because of stronger-than-expected demand for green bonds.

To verify whether the performance of green bonds relative to conventional bonds is driven by the flow of information described above, in Figure 12 we recompute the expected green excess returns for the first pair of twin bonds starting from after the German floods (September 2021), rather than from the time of issuance (September 2020) as in the top left panel of Figure 11. In other words, we ask ourselves how the expected green excess returns change once investors learn about the 2021 Climate Change Act and the German floods and choose

---

<sup>16</sup>Holding both bonds to maturity still leads to zero or negative green excess returns.

<sup>17</sup>Differently from equities, the sovereign green bonds we consider are not an effective hedge against climate risks, because their cash-flows are fixed ex ante. Any increase in price from heightened climate concerns must be temporary, as regardless of the value of the green factor  $G_t$ , the green spread must converge to zero as the bonds mature.

<sup>18</sup>On April 29, 2021, the Federal Constitutional Court (Germany’s highest court) rules that the 2019 Climate Change Act was unconstitutional because of generational equity violation. Even if the German government had until the end of 2022 to amend the 2019 Climate Change Act, on May 12, 2021, Germany’s federal cabinet adopts the reforms to the 2019 Climate Change Act, that is, the 2021 Climate Change Act shifts to a net-zero target by 2045. See The Economist “A court ruling triggers a big change in Germany’s climate policy”; POLITICO “Top German court rules the country’s climate law is partly ‘unconstitutional’”; Reuters “Germany sets tougher CO2 emission reduction targets after top court ruling.”

to hold green bonds.

The left panel of Figure 12 shows that after the German floods, expected green excess returns are negative, as predicted by Pastor, Stambaugh and Taylor (2021). Furthermore, realized returns are still a bit higher for the first 6 months, but then sink below the expected returns following the beginning of the Ukrainian war in February 2022. The unexpected invasion of Ukraine most likely pushed investors toward the more liquid conventional bonds, which is typical during flight-to-quality episodes. For this reason, the right panel of Figure 12 shows the expected green excess returns for the same pair of twin bonds, but computed starting in March 2022, soon after the invasion of Ukraine. In this case, again the expected green excess returns are negative, and the green bonds perform worse than expected because of the flight-to-quality to conventional securities. This is consistent with the green spread shrinking due to confounding factors unrelated to environmental preferences.

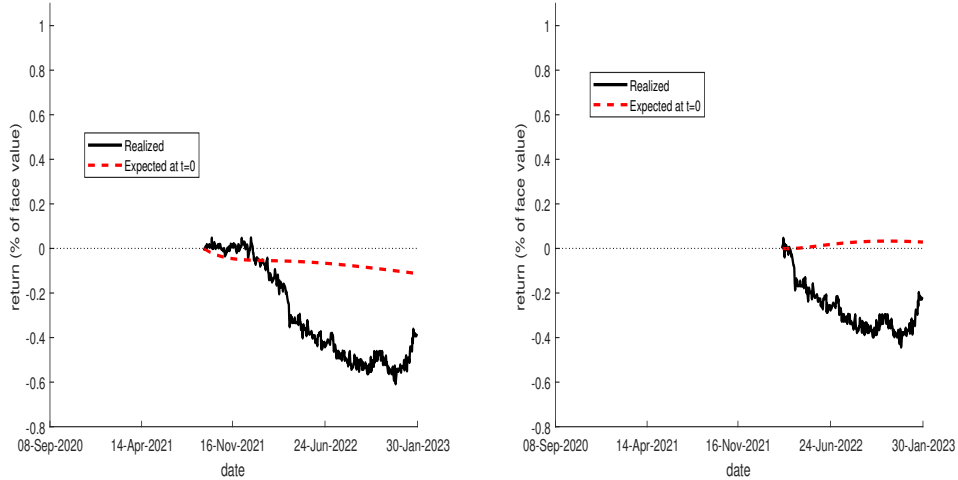


**Figure 12.** Realized and Expected Excess Returns on German Twins

Both panels plot realized and expected excess returns on the first German twin pair. The left panel plots realized and expected returns starting from September 9, 2021 (after the German floods) while the right panel plots realized and expected returns starting from March 1, 2022 (after the start of the war in Ukraine).

Figure 13 explores the dynamics and term structure of the model's implied expected green excess returns, which we define for a fixed maturity  $\tau$  and a fixed horizon  $h$  as

$$E_t \left\{ R_{t+h}^{(\tau)} \right\} \equiv E_t \left\{ P_{t+h}^g(\tau - h) - P_{t+h}(\tau - h) \right\} - [P_t^g(\tau) - P_t(\tau)]. \quad (16)$$

In contrast to equation (15) and Figure 11, equation (16) holds both the maturity  $\tau$  and the horizon  $h$  fixed; what varies instead is time  $t$ . Figure 13 plots equation (16) over time,

for zero-coupon bonds with 5, 10, and 30 years to maturity and a fixed 1-month investment horizon. This is meant to illustrate one of the possible forecasting exercises that can be conducted with our DTSM.

Figure 13 shows that the model-implied expected 1-month green excess returns can be either positive or negative, can change quite rapidly, and have been decreasing steadily over the sample—as the benchmark greenium has gotten larger (Figure 8). Early in the sample—when there are fewer green bonds, and green spreads are widening—expected green excess returns are positive, though not constant. In mid-2021, after Germany issues its 30-year green bond but before the 10-year green spread begins to narrow (Figure 8), expected excess green returns briefly flip to negative and then bounce back. Around March 2022—e.g., after the beginning of the war in Ukraine—expected excess 1-month green returns turn into negative territory, where they remain until the end of the sample.

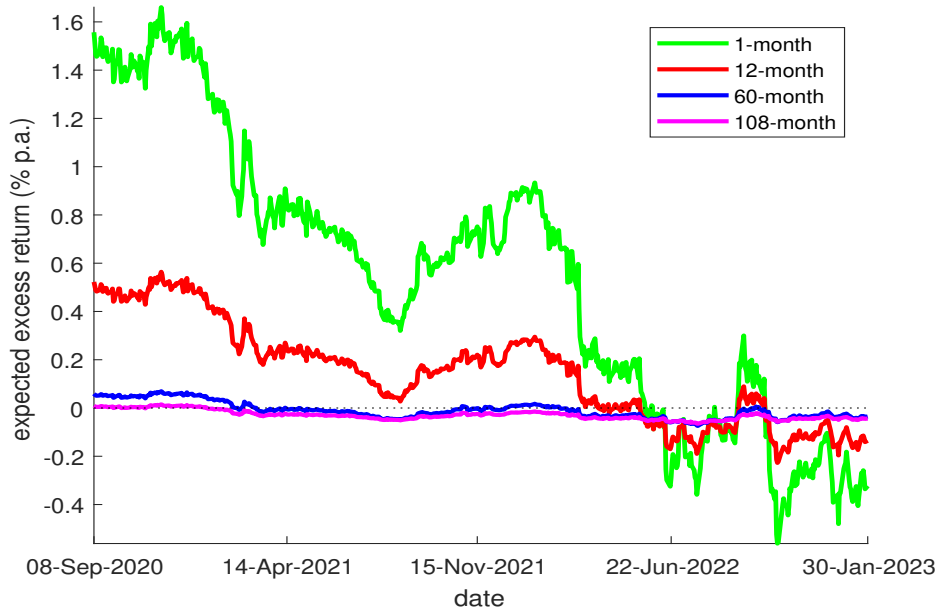


**Figure 13.** Expected Excess Green Returns

The figure plots the model-implied annualized 1-month expected excess returns from equation (16) for synthetic zero-coupon bonds with 5, 10, and 30 years to maturity.

## 6 Conclusion

We estimate the benchmark greenium by exploiting the unique “twin” structure of German sovereign green bonds. Since the simple yield spread between a green security and its conventional twin (i.e., the green spread) can be contaminated by idiosyncratic and confounding

factors unrelated to climate/environmental concerns, we use a DTSM that jointly prices green and conventional bonds. The model, by estimating the systemic conventional factors driving all bond prices as well as a green factor specific to green bonds, allows us to eliminate temporary mispricing due to idiosyncratic and confounding factors such as relative scarcity induced by flight-to-quality or small issuance size of green bonds. In this sense, the model delivers an estimate of the “fundamental” greenium: the dividend investors are willing to forego to subsidize the government’s green projects.

Indeed, we find that, differently from the simple green spread, the model-implied greenium is uncorrelated with confounding and idiosyncratic factors. The time-series fluctuations of the estimated greenium are significantly related to major environmental events, while the green spread is mostly driven by factors capturing financial motives, such as stock market prices and measures of flight-to-quality and liquidity. Hence, our estimates of the greenium provide a cleaner measure of the subsidy investors are willing to provide the government to finance adaptation and mitigation projects. The purified greenium also gives a clearer signal about investors’ environmental preferences to policy makers currently considering to broaden support for sustainable finance by, for example, including green bonds in the implementation of fiscal and monetary policies.

Further, estimating a DTSM enhances our understanding of the greenium beyond the simple green spread in three ways. First, the greenium is larger than the raw green spread, highlighting the importance of controlling for security-level mispricing. Second, the model-implied term structure of the greenium is upward sloping, in contrast to the term structure of green spreads which is downward sloping. The greenium’s upward-sloping term structure is more in line with the horizon of the government’s climate goals, which will require increasing green investments to transition to net zero emissions by 2045. Third, the model allows us to estimate expected returns at all horizons, while green spreads offer only a measure of realized returns and expected returns holding to maturity.

Our estimated expected green excess return (i.e., the difference between expected green and conventional returns) varies with the investment horizon and investors’ information set, as it is positive at issuance (September 2020) and turns negative after the German floods (July 2021). In line with [Pastor, Stambaugh and Taylor \(2021\)](#), as investors become more concerned about the environment, they are willing to accept lower returns to hold green assets. Further, as suggested by [Pastor, Stambaugh and Taylor \(2022\)](#), the expected and realized green excess returns diverge when there is an unanticipated increase in climate concerns; but, they also diverge when there are surprises unrelated to environmental preferences, such as the start of the Ukrainian war that triggered flight-to-quality to German conventional securities. This finding is consistent with a green spread that, differently from the

greenium, is contaminated by confounding risk factors.

In the future, our estimates could inform an analysis of the relationship between the primary and secondary market for green bonds, in order to better connect the high demand for green bonds at auction with the dynamics of the subsequent greenium in the secondary market. For instance, Pietsch and Salakhova (2022) find that, in Europe, the greenium for corporate bonds gets larger when the share held by retail investors increases relative to the share of Investment Funds, Insurance Companies and Pension Funds. Finally, our methodology can be used to estimate the greenium for other countries, including France and the UK, that issue green bonds but do not pair them directly with a conventional “twin.”

# A Proofs

## A.1 Proof of Proposition 1

*Proof.* Define

$$\tilde{X}_t \equiv \begin{bmatrix} X_t \\ G_t \end{bmatrix}$$

and note that equations (2) and (3) imply that

$$d\tilde{X}_t = \left[ -\mu - \phi\tilde{X}_t \right] dt + \Sigma d\tilde{W}_t$$

where

$$\begin{aligned} W_t &\equiv \begin{bmatrix} W_t^x \\ W_t^g \end{bmatrix} \\ \mu &\equiv \begin{bmatrix} \mu_x \\ \mu_g \end{bmatrix} \\ \phi &\equiv \begin{bmatrix} \phi_x & \vec{0} \\ \vec{0} & \phi_g \end{bmatrix} \\ \Sigma &\equiv \begin{bmatrix} \Sigma_x & \vec{0} \\ \vec{0} & \Sigma_g \end{bmatrix}. \end{aligned}$$

Similarly, equation (4) can be rewritten as

$$\frac{dM_t}{M_t} = - \left[ \delta_0 + \tilde{\delta}'_1 \tilde{X}_t \right] dt - \left[ \sigma \left( \tilde{X}_t \right) - \Sigma^{-1} \tilde{X}_t \tilde{X}'_t \tilde{\delta}_1 \right] \cdot d\tilde{W}_t$$

where  $\tilde{\delta}_1 \equiv [\delta'_1, 0]'$  and  $\sigma \left( \tilde{X}_t \right) = \sigma \left( X_t, G_t \right)$ .

Assuming a solution of the form (10) and applying Ito's lemma to the above equations



and equation (6) gives

$$\begin{aligned}
0 &= -\frac{\partial \tilde{A}^g}{\partial \tau} - \frac{\partial \tilde{B}^{g'}}{\partial \tau} \tilde{X}_t - \left( \tilde{A}^g(\tau) + \tilde{B}^g(\tau)' \tilde{X}_t \right) \left( \delta_0 + \tilde{\delta}'_1 \tilde{X}_t \right) \\
&\quad + \tilde{B}^g(\tau)' \left[ -\tilde{\mu}^* - \tilde{\phi}^* X_t + \Sigma \sigma \left( \tilde{X}_t \right) \right] \\
&\quad - \tilde{B}^g(\tau)' \Sigma \left[ \sigma \left( \tilde{X}_t \right) - \Sigma^{-1} \tilde{X}_t \tilde{X}_t' \tilde{\delta}_1 \right] - \delta'_g \tilde{X}_t \left( \delta_0 + \tilde{\delta}'_1 \tilde{X}_t \right) \\
&\quad + \delta'_g \left( -\tilde{\mu}^* - \tilde{\phi}^* \tilde{X}_t + \Sigma \sigma \left( X_t \right) \right) - \delta'_g \Sigma \left[ \sigma \left( \tilde{X}_t \right) - \Sigma^{-1} \tilde{X}_t \tilde{X}_t' \tilde{\delta}_1 \right] \\
&= -\frac{\partial \tilde{A}^g}{\partial \tau} - \tilde{A}^g(\tau) \delta_0 - \left( \tilde{B}^g(\tau) + \delta_g \right)' \tilde{\mu}^* - \frac{\partial \tilde{B}^{g'}}{\partial \tau} \tilde{X}_t - \tilde{A}^g(\tau) \tilde{\delta}'_1 \tilde{X}_t - \left( \tilde{B}^g(\tau) + \delta_g \right)' \left( \delta_0 I + \tilde{\phi}^* \right) \tilde{X}_t
\end{aligned} \tag{17}$$

where  $\delta_g \equiv \left[ \vec{0}_{1 \times k}, 1 \right]'$ .

Because equation (17) must hold for all values of  $\tilde{X}_t$ , it must be that  $\tilde{A}^g(\tau)$  and  $\tilde{B}^g(\tau)$  satisfy the system of ordinary differential equations

$$\begin{aligned}
\frac{\partial \tilde{A}^g}{\partial \tau} &= -\delta'_g \tilde{\mu}^* - \tilde{A}^g(\tau) \delta_0 - \tilde{B}^g(\tau)' \tilde{\mu}^* \\
\frac{\partial \tilde{B}^{g'}}{\partial \tau} &= -\delta'_g \left( \tilde{\phi}^* + \delta_0 I \right) - \tilde{A}^g(\tau) \tilde{\delta}'_1 - \tilde{B}^g(\tau)' \left( \tilde{\phi}^* + \delta_0 I \right),
\end{aligned} \tag{18}$$

with initial conditions  $\tilde{A}^g(0) = 1$  and  $\tilde{B}^g(0) = \vec{0}_{k+1 \times 1}$ . Equation (11) is the solution of this system, where the top row is the constant function  $f(\tau) = 1$  and subsequent rows have been converted from  $\tilde{X}_t$  to  $\{X_t, G_t\}$  notation.

Equation (8) can be derived as a special case with  $\mu_g^* = \phi_g^* = 0$  and  $\delta_g = \vec{0}$ .

## B Estimation Details

In this section we describe in more detail how we estimate the model of Section 3.1 on the data.

We estimate the models using the SR filter of [Andreasen and Christensen \(2015\)](#), which consists of a two-stage procedure: first, we estimate the risk-neutral parameters  $\theta^*$  and the latent factors  $X_t$  and  $G_t$  as described below in Section B.1. Denote the estimated values of  $X_t$  and  $G_t$  as  $\hat{X}_t$  and  $\hat{G}_t$ , respectively, so that

$$\begin{aligned}
\hat{X}_t &= X_t + \nu_t^x \\
\hat{G}_t &= G_t + \nu_t^g.
\end{aligned} \tag{19}$$

where  $\nu_t^x$  and  $\nu_t^g$  are sampling errors from the filter. In the first step, we recover the daily covariance matrices  $\Xi_t^x$  and  $\Xi_t^g$  of  $\nu_t^x$  and  $\nu_t^g$ . In the second step, described below in Section B.2, we use these covariance matrices to estimate the time-series parameters of the model, accounting for the estimation of the latent factors and the risk-neutral parameters themselves. To do so, we discretize equations (2) and (3) and treat the time-series side of the model as a pair of daily vector autoregressions.

To estimate both conventional and green bond prices, accounting for the fact that our samples consists of 166,680 price observations on 159 conventional bonds from October 27, 2008 to August 30, 2022 and 1,525 price observations on 4 green bonds from September 8, 2020 to August 30, 2022, we proceed in steps. First, we estimate  $\delta_0$  and  $\mu^*$  using the longer conventional bond sample only. We then estimate  $\mu_g^*$  and  $\phi_g^*$  using all bonds, but only the sample starting in September 2020, and holding  $\delta_0$  and  $\mu^*$  fixed. Finally, we estimate all the risk-neutral parameters jointly over the entire sample using the previous two estimates as an initial guess.<sup>19</sup>

Once we have the seven risk-neutral parameters and the associated estimates for the latent factors, we then estimate the time-series parameters and all standard errors. Table 5 reports the estimated parameters, with standard errors below each value in parentheses.

## B.1 Risk-Neutral Parameters

The risk-neutral estimation is a nonlinear least squares (NLLS) problem in the risk-neutral parameters  $\theta^*$ , where the latent factors are nuisance parameters. Given  $\theta^*$ , we construct the measurement matrices of equation (13) on each date using the coupon schedule of each bond and the factor loadings of equations (8) and (11). We then estimate  $\hat{X}_t$  and  $\hat{G}_t$  on each date using equation (13), and compute the total sum of squared residuals across all dates. Finally, we search over values of  $\theta^*$  to minimize this sum of squared residuals.

The standard errors of  $\theta^*$  correspond to the usual NLLS standard errors. Let

$$\mathbb{X}_i \equiv \begin{bmatrix} \frac{\partial \hat{P}_i}{\partial \theta_1^*} & \frac{\partial \hat{P}_i}{\partial \theta_2^*} & \cdots & \frac{\partial \hat{P}_i}{\partial \theta_k^*} \end{bmatrix} \quad (20)$$

denote the vector of derivatives of the  $i$ th estimated bond price with respect to the  $k$  risk-neutral parameters, including the parameters that affect green bond prices. For observations  $i$  before the introduction of green bonds we set the relevant elements of  $\mathbb{X}_i$  to zero. We approximate Equation (20) using a complex-step derivative with step size  $10^{-12}$ .

---

<sup>19</sup>Because there are only four green bonds and only for a short part of the sample, and because the green bond parameters have no effect on conventional bonds, the parameter estimates in the third step are nearly identical to the initial guess.

$\delta_0$		$\mu^{*'} $		
0.00157 (1.54e-17)	-1.78e-06 (-2.77e-20)	5.61e-10 (2.63e-23)	-1.17e-13 (-1.35e-26)	1.55e-18 (3e-30)
$\mu$		$\phi$		
-1.02e-05 (7.17e-06)	-0.00486 (0.00276)	-0.000183 (0.00275)	7.95e-05 (0.00205)	0.00257 (0.00319)
1.19e-05 (1.66e-05)	0.000787 (0.00613)	-0.0149 (0.00651)	0.00904 (0.00454)	0.0172 (0.00717)
-9.1e-06 (1.99e-05)	-6.59e-06 (0.00743)	0.00905 (0.00782)	-0.00754 (0.00584)	-0.00932 (0.00908)
1.15e-05 (1.66e-05)	0.00158 (0.00616)	-0.00889 (0.00648)	0.00536 (0.00479)	0.00794 (0.00742)
$\Sigma_x \Sigma'_x$				
	9.03e-13 (2.7e-13)	-9.43e-13 (3.26e-13)	5.7e-13 (3.94e-13)	-6.89e-13 (3.27e-13)
	-9.43e-13 (3.26e-13)	4.39e-12 (1.58e-12)	-4.16e-12 (9.55e-13)	4.02e-12 (7.94e-13)
	5.7e-13 (3.94e-13)	-4.16e-12 (9.55e-13)	6.74e-12 (2.31e-12)	-5.19e-12 (9.6e-13)
	-6.89e-13 (3.27e-13)	4.02e-12 (7.94e-13)	-5.19e-12 (9.6e-13)	4.55e-12 (1.6e-12)
$\mu_g^*$	$\phi_g^*$	$\mu_g$	$\phi_g$	$\Sigma_g^2$
-6.63e-06 (1.16e-12)	-0.000115 (2.9e-12)	-0.000604 (0.000193)	-0.0123 (0.0037)	5.76e-08 (2.86e-08)

**Table 5.** Parameter Estimates

The table reports the estimated parameters of the model described in Section 3.1. The top panel reports the risk-neutral parameters that affect all bonds, the second panel reports the time-series parameters  $\mu$  and  $\phi$  for the conventional factors  $X_t$ , while the third panel reports the variance-covariance matrix of the conventional factor time-series residuals. The bottom panel reports both the risk-neutral and time-series parameters affecting green bonds.

Let  $\mathbb{X}_t$  denote the  $n_t \times k$  matrix of stacked derivatives, for the  $n_t$  price observations at  $t$ , and let  $\mathbb{X}$  be the  $N \times k$  stacked derivatives across all cross-sections, where  $N = 166,680$ . Then the asymptotic covariance matrix of  $\theta^*$  is given by

$$\text{asymVar}(\theta^*) = \frac{1}{N} \left( A^{\theta^*} \right)^{-1} B^{\theta^*} \left( A^{\theta^*} \right)^{-1}, \quad (21)$$

where

$$\begin{aligned} A^{\theta^*} &\equiv \frac{1}{N} \mathbb{X}' \mathbb{X} \\ B^{\theta^*} &\equiv \frac{1}{N} \mathbb{X}' \Sigma_M \mathbb{X} \end{aligned}$$

and

$$\begin{aligned} \Sigma_M &= \text{diag} \left\{ \hat{\Sigma}_t^M \right\} \\ \hat{\Sigma}_t^M &\equiv \frac{1}{n_t} \sum_{i=1}^{n_t} \hat{\varepsilon}_{i,t}^2 \end{aligned}$$

is the maximum-likelihood estimator of the specification-error variance in Equation (13), diagonalized to have the proper dimensionality.

## B.2 Time-Series Parameters

While the risk-neutral parameter estimation is a relatively straightforward NLLS exercise, estimating the time-series parameters requires a bit more work. In particular, in the second step we need to account for both the sampling error in the latent factors, as well as the sampling error in the risk-neutral parameters themselves.

First, we discretize the time-series equations (2) and (3) as

$$\begin{aligned} Y_{t+\Delta_t} &\equiv \frac{X_{t+\Delta_t} - X_t}{\sqrt{\Delta_t}} \approx \mu_x \sqrt{\Delta_t} + \phi_x \sqrt{\Delta_t} X_t + \Sigma_x \frac{W_{t+\Delta_t}^x}{\sqrt{\Delta_t}} \\ Y_{t+\Delta_t}^g &\equiv \frac{G_{t+\Delta_t} - G_t}{\sqrt{\Delta_t}} \approx \mu_g \sqrt{\Delta_t} + \phi_g \sqrt{\Delta_t} G_t + \Sigma_g \frac{W_{t+\Delta_t}^g}{\sqrt{\Delta_t}}. \end{aligned} \quad (22)$$

If the latent factors were observable without error, Equation (22) could be estimated

directly using ordinary least squares; in this case, the moment conditions are

$$\begin{aligned}
E \{W_{t+\Delta_t}^x\} &= \vec{0} & E \{W_{t+\Delta_t}^g\} &= 0 \\
E \{W_{t+\Delta_t}^x X_t'\} &= \vec{0} & E \{W_{t+\Delta_t}^g G_t\} &= 0 \\
E \{W_{t+\Delta_t}^x W_{t+\Delta_t}^{x'}\} &= \Sigma_x \Sigma_x' & E \left\{ \left( W_{t+\Delta_t}^g \right)^2 \right\} &= \Sigma_g^2.
\end{aligned} \tag{23}$$

However, because the latent factors are estimated with error (equation 19), the empirical analog of Equation (23) cannot be implemented directly. Instead, we have that

$$\begin{aligned}
\hat{W}_{t+\Delta_t}^x &= \frac{\hat{Y}_{t+\Delta_t}}{\sqrt{\Delta_t}} - \sqrt{\Delta_t} \left( \mu_x + \phi_x \hat{X}_t \right) \\
&= W_{t+\Delta_t}^x + \frac{\nu_{t+\Delta_t}^x - \nu_t^x}{\sqrt{\Delta_t}} - \sqrt{\Delta_t} \phi_x \nu_t^x \\
\hat{W}_{t+\Delta_t}^x \hat{X}_t' &= \left( W_{t+\Delta_t}^x + \frac{\nu_{t+\Delta_t}^x - \nu_t^x}{\sqrt{\Delta_t}} - \sqrt{\Delta_t} \phi_x \nu_t^x \right) (X_t + \nu_t^x)' \\
\hat{W}_{t+\Delta_t}^x \hat{W}_{t+\Delta_t}^{x'} &= \left( W_{t+\Delta_t}^x + \frac{\nu_{t+\Delta_t}^x - \nu_t^x}{\sqrt{\Delta_t}} - \sqrt{\Delta_t} \phi_x \nu_t^x \right) \left( W_{t+\Delta_t}^x + \frac{\nu_{t+\Delta_t}^x - \nu_t^x}{\sqrt{\Delta_t}} - \sqrt{\Delta_t} \phi_x \nu_t^x \right)',
\end{aligned} \tag{24}$$

for the conventional factors  $X_t$ , and a parallel equation for the green factor  $G_t$ . Taking expectations of Equation (24), armed with the variance of  $\nu_t^x$ ,  $\Xi_t^x$ , and its covariance with  $\nu_{t+\Delta_t}^x$  (the calculation of both of which we describe in further detail below), leads to the usable moment conditions

$$\begin{aligned}
E \{ \hat{W}_{t+\Delta_t}^x \} &= \vec{0} \\
E \{ \hat{W}_{t+\Delta_t}^x \hat{X}_t' \} &= \frac{\text{cov} \{ \nu_{t+\Delta_t}^x, \nu_t^x \}}{\sqrt{\Delta_t}} - \underbrace{\left( \frac{I}{\sqrt{\Delta_t}} + \sqrt{\Delta_t} \phi_x \right)}_{\equiv \Phi_t^x} \Xi_t^x \\
E \{ \hat{W}_{t+\Delta_t}^x \hat{W}_{t+\Delta_t}^{x'} \} &= \Sigma_x \Sigma_x' + \frac{\Xi_{t+1}^x}{\Delta_t} + \Phi_t^x \Xi_t^x \Phi_t^{x'} - \frac{\text{cov} \{ \nu_{t+\Delta_t}^x, \nu_t^x \}}{\sqrt{\Delta_t}} \Phi_t^{x'} - \Phi_t^x \frac{\text{cov} \{ \nu_{t+\Delta_t}^x, \nu_t^x \}}{\sqrt{\Delta_t}},
\end{aligned}$$

where the second line defines the matrix  $\Phi_t^x$ , and a similar equation holds for the green factor

$G_t$ . Define

$$\begin{aligned}
q_t^x &\equiv \begin{bmatrix} \hat{W}_{t+\Delta_t}^x \\ \text{vec} \left\{ \hat{W}_{t+\Delta_t}^x \hat{X}_t' - \frac{\text{cov}\{\nu_{t+\Delta_t}^x, \nu_t^x\}}{\sqrt{\Delta_t}} + \Phi_t^x \Xi_t^x \right\} \\ \text{vech} \left\{ \hat{W}_{t+\Delta_t}^x \hat{W}_{t+\Delta_t}^{x'} - \Sigma_x \Sigma_x' - \frac{\Xi_{t+1}^x}{\Delta_t} - \Phi_t^x \Xi_t^x \Phi_t^{x'} \right. \\ \left. + \frac{\text{cov}\{\nu_{t+\Delta_t}^x, \nu_t^x\}}{\sqrt{\Delta_t}} \Phi_t^{x'} + \Phi_t^x \frac{\text{cov}\{\nu_{t+\Delta_t}^x, \nu_t^x\}}{\sqrt{\Delta_t}} \right\} \end{bmatrix} \\
q_t^g &\equiv \begin{bmatrix} \hat{W}_{t+\Delta_t}^g \\ \hat{W}_{t+\Delta_t}^g \hat{G}_t - \frac{\text{cov}\{\nu_{t+\Delta_t}^g, \nu_t^g\}}{\sqrt{\Delta_t}} + \Phi_t^g \Xi_t^g \\ \left( \hat{W}_{t+\Delta_t}^g \right)^2 - \Sigma_g^2 - \frac{\Xi_{t+1}^g}{\Delta_t} - \left( \Phi_t^g \right)^2 \Xi_t^g + 2 \frac{\text{cov}\{\nu_{t+\Delta_t}^g, \nu_t^g\}}{\sqrt{\Delta_t}} \Phi_t^g \end{bmatrix}. \tag{25}
\end{aligned}$$

Then, our time series estimates of the parameters in equations (2) and (3) are those that set  $\sum_t q_t^x = \sum_t q_t^g = 0$  in sample.

To compute the standard errors of the time-series parameters, we must compute the variance matrices of the measurement errors  $\Xi_t^x$  and  $\Xi_t^g$ , as well as the covariances of the measurement errors over time. To do so, we follow [Andreasen and Christensen \(2015\)](#) and account for the latency of the factors  $X_t$  from two sources: (1) sampling variation at  $t$ , and (2) sampling variation in  $\theta^*$  itself (and through it, the factor loadings). We compute

$$\Xi_t = \frac{1}{n_t} A_t^{-1} V_t A_t^{-1},$$

where

$$\begin{aligned}
A_t &= \frac{1}{n_t} J_t' J_t \\
J_t &= \frac{\partial \hat{P}_{it}}{\partial X_t}
\end{aligned}$$

and

$$\begin{aligned}
V_t &= B_t + \sqrt{\frac{n_t}{N}} C_t \left( A^{\theta^*} \right)^{-1} \left( \sqrt{\frac{n_t}{N}} B^{\theta^*} \left( A^{\theta^*} \right)^{-1} - 2 \hat{\Sigma}_t^M \right) C_t' \\
B_t &= \hat{\Sigma}_t^M A_t \\
C_t &= \frac{1}{n_t} J_t' \mathbb{X}_t,
\end{aligned}$$

and then define  $\Xi_t^x$  as the upper-left  $4 \times 4$  block of  $\Xi_t$ , and  $\Xi_t^g$  as the lower-right element of  $\Xi_t$ . Note that the latter is undefined in the early sample before green bonds are issued; for these values of  $t$ ,  $\Xi_t$  is a  $4 \times 4$  matrix. Likewise, in the early sample the  $J_t$  matrices are the second through fifth columns of the measurement matrix in equation (13); in the later sample including green bonds, the  $J_t$  matrices are the second through sixth columns of the measurement matrix.

Finally, to compute  $\text{cov} \{ \nu_{t+\Delta_t}^x, \nu_t^x \}$  and  $\text{cov} \{ \nu_{t+\Delta_t}^g, \nu_t^g \}$ , we estimate a daily AR(1) on the realized bond-level residuals:

$$\frac{\eta_{i,t+\Delta_t}}{\sqrt{\Delta_t}} = \rho \eta_{i,t} \sqrt{\Delta_t} + \frac{\varepsilon_{i,t+\Delta_t}^m}{\sqrt{\Delta_t}},$$

where the variance of  $\varepsilon_{i,t+\Delta_t}^m$  is  $\Delta_t \sigma_m^2$  and the  $\sqrt{\Delta_t}$  terms correct for the varying number of days between observations in the sample. On each date, we use the estimated values of  $\rho$  and  $\sigma_m^2$  to construct the  $n_{t+\Delta_t} \times n_t$  matrix of bond-level measurement error autocovariances  $\Sigma_{t+\Delta_t,t}$ , with  $(i, j)$  element given by

$$(\Sigma_{t+\Delta_t,t})_{ij} \equiv \begin{cases} \rho^{\Delta_t} \frac{\sigma_m^2}{1-\rho^2} & \text{if bond } i \text{ at } t + \Delta_t \text{ is the same CUSIP as bond } j \text{ at } t \\ 0 & \text{otherwise} \end{cases}$$

We then construct

$$\text{c}\hat{\text{ov}} \{ \nu_{t+\Delta_t}, \nu_t \} = \frac{1}{n_{t+\Delta_t}} \frac{1}{n_t} A_{t+\Delta_t}^{-1} J'_{t+\Delta_t} \Sigma_{t+\Delta_t,t} J_t A_t^{-1}$$

and define  $\text{c}\hat{\text{ov}} \{ \nu_{t+\Delta_t}^x, \nu_t^x \}$  as the upper  $4 \times 4$  block of  $\text{c}\hat{\text{ov}} \{ \nu_{t+\Delta_t}, \nu_t \}$ , while  $\text{c}\hat{\text{ov}} \{ \nu_{t+\Delta_t}^g, \nu_t^g \}$  is the lower-right element of the same matrix.

Finally, I estimate the standard errors of the time-series parameters  $\{ \mu_i, \phi_i, \Sigma_i \Sigma_i' \}$  where  $i \in \{x, g\}$ , as the usual GMM standard errors, accounting for  $\Xi_t^i$ :

$$\text{asymVar}(\theta_i) = \frac{1}{T_i} (R_i S_i^{-1} R_i')^{-1},$$

where

$$S_i \equiv \frac{1}{T_i - 1} \sum_{t=1}^{T_i} q_t^i q_t^{i'}$$

$$R_i \equiv \frac{1}{T_i - 1} \sum_{t=1}^{T_i} \frac{\partial q_t^i}{\partial \theta_i}$$

and  $q_t^i$  is defined in Equation (25). Notice that this procedure accounts for the different number of time-series observations in the green and conventional samples.



## References

- Alekseev, Georgij, Stefano Giglio, Quinn Maingi, Julia Selgrad, and Johannes Stroebel.** 2021. “A quantity-based approach to constructing climate risk hedge portfolios.” *Working Paper*. 6
- Andreasen, Martin M., and Bent Jesper Christensen.** 2015. “The SR Approach: A New Estimation Procedure For Non-Linear And Non-Gaussian Dynamic Term Structure Models.” *Journal of Econometrics*, 184(2): 420–451. 20, 41, 46
- Baker, Malcolm, Daniel Bergstresser, George Serafeim, and Jeffrey Wurgler.** 2018. “Financing The Response To Climate Change: The Pricing And Ownership Of U.S. Green Bonds.” National Bureau of Economic Research Working Paper 25194. 5
- Bansal, Ravi, Dana Kiku, and Marcelo Ochoa.** 2016. “Price of long-run temperature shifts in capital markets.” National Bureau of Economic Research. 6
- Bauer, Michael D, and Glenn D Rudebusch.** 2021. “The rising cost of climate change: evidence from the bond market.” *The Review of Economics and Statistics*, 1–45. 6
- Berardi, Andrea, Roger Brown, and Stephen M Schaefer.** 2021. “Bond risk premia: The information in (really) long term rates.” *Working Paper*. 21
- Berg, Florian, Julian F Kölbel, Anna Pavlova, and Roberto Rigobon.** 2021. “ESG Confusion and Stock Returns: Tackling the Problem of Noise.” *Working Paper*. 5, 9
- Bernstein, Asaf, Matthew T Gustafson, and Ryan Lewis.** 2019. “Disaster on the horizon: The price effect of sea level rise.” *Journal of financial economics*, 134(2): 253–272. 6
- Cevik, Serhan, and João Tovar Jalles.** 2022. “An apocalypse foretold: Climate shocks and sovereign defaults.” *Open Economies Review*, 33(1): 89–108. 6
- Chikhani, Pauline, and Jean-Paul Renne.** 2022. “Climate Linkers: Rationale and Pricing.” *Available at SSRN 3881262*. 6
- Cochrane, John H., and Monika Piazzesi.** 2008. “Decomposing the Yield Curve.” *Working paper*. 21
- Colombage, Sisira, and KGM Nanayakkara.** 2020. “Impact of credit quality on credit spread of Green Bonds: a global evidence.” *Review of Development Finance*, 10(1): 31–42. 5

- D’Amico, Stefania, and N Aaron Pancost.** 2021. “Special Repo Rates and the Cross-Section of Bond Prices: The Role of the Special Collateral Risk Premium.” *Review of Finance*, 26(1): 117–162. 16
- D’Amico, Stefania, Don H. Kim, and Min Wei.** 2018. “Tips From TIPS: The Informational Content Of Treasury Inflation-Protected Security Prices.” *Journal of Financial and Quantitative Analysis*, 53(1): 395–436. 10
- Deutsche Finanzagentur.** 2022. “Federal Republic of Germany Green Bond Investor Presentation.” *presentation slides*. 12
- Duffie, Darrell.** 1996. “Special Repo Rates.” *The Journal of Finance*, 51(2): 493–526. 16
- Engle, Robert F, Stefano Giglio, Bryan Kelly, Heebum Lee, and Johannes StroebeL.** 2020. “Hedging climate change news.” *The Review of Financial Studies*, 33(3): 1184–1216. 6
- Flammer, Caroline.** 2020. “Green bonds: effectiveness and implications for public policy.” *Environmental and Energy Policy and the Economy*, 1(1): 95–128. 5
- Flammer, Caroline.** 2021. “Corporate green bonds.” *Journal of Financial Economics*, 142(2): 499–516. 5
- Gabaix, Xavier.** 2007. “Linearity-Generating Processes: A Modelling Tool Yielding Closed Forms For Asset Prices.” National Bureau of Economic Research Working Paper 13430. 17
- Gabaix, Xavier.** 2008. “Variable Rare Disasters: A Tractable Theory of Ten Puzzles in Macro-Finance.” *The American Economic Review*, 98(2): 64–67. 17
- Giglio, Stefano, Matteo Maggiori, Krishna Rao, Johannes StroebeL, and Andreas Weber.** 2021. “Climate change and long-run discount rates: Evidence from real estate.” *The Review of Financial Studies*, 34(8): 3527–3571. 6
- Huynh, Thanh D, and Ying Xia.** 2021. “Climate change news risk and corporate bond returns.” *Journal of Financial and Quantitative Analysis*, 56(6): 1985–2009. 6
- Ilhan, Emirhan, Zacharias Sautner, and Grigory Vilkov.** 2021. “Carbon tail risk.” *The Review of Financial Studies*, 34(3): 1540–1571. 6
- Kapraun, Julia, Carmelo Latino, Christopher Scheins, and Christian Schlag.** 2021. “(In)-credibly green: which bonds trade at a green bond premium?” 5

- Karpf, Andreas, and Antoine Mandel.** 2018. “The changing value of the greenlabel on the US municipal bond market.” *Nature Climate Change*, 8(2): 161–165. 5
- Kling, Matthew M, Stephanie L Auer, Patrick J Comer, David D Ackerly, and Healy Hamilton.** 2020. “Multiple axes of ecological vulnerability to climate change.” *Global Change Biology*, 26(5): 2798–2813. 6
- Krueger, Philipp, Zacharias Sautner, and Laura T Starks.** 2020. “The importance of climate risks for institutional investors.” *The Review of Financial Studies*, 33(3): 1067–1111. 6
- Larcker, David F., and Edward M. Watts.** 2020. “Where’s The Greenium?” *Journal of Accounting and Economics*, 69(2): 0–101312. 5
- Litterman, Robert, and Jose Scheinkman.** 1991. “Common factors affecting bond returns.” *Journal of fixed income*, 1(1): 54–61. 21
- Oehmke, Martin, and Marcus M Opp.** 2022. “Green Capital Requirements.” *Available at SSRN*. 6
- Painter, Marcus.** 2020. “An inconvenient cost: The effects of climate change on municipal bonds.” *Journal of Financial Economics*, 135(2): 468–482. 6
- Pancost, N. Aaron.** 2021. “Zero-Coupon Yields and the Cross-Section of Bond Prices.” *The Review of Asset Pricing Studies*, 11(2): 209–268. 4, 19, 20
- Papoutsis, Melina, Monika Piazzesi, and Martin Schneider.** 2021. “How unconventional is green monetary policy.” *JEEA-FBBVA Lecture at the ASSA (January)*. 6
- Pastor, Lubos, Robert F. Stambaugh, and Lucian A. Taylor.** 2021. “Sustainable Investing In Equilibrium.” *Journal of Financial Economics*, 142(2): 550–571. 4, 5, 9, 34, 36, 38
- Pastor, Lubos, Robert F. Stambaugh, and Lucian A. Taylor.** 2022. “Dissecting green returns.” *Journal of Financial Economics*, 146(2): 403–424. 5, 38
- Riedler, Jesper, and Tina Koziol.** 2021. “Scaling, unwinding and greening QE in a calibrated portfolio balance model.” *ZEW Discussion Papers*, 21. 6
- Semmler, Willi, Joao Paulo Braga, Andreas Lichtenberger, Marieme Toure, and Erin Hayde.** 2021. “Fiscal policies for a low-carbon economy.” 6

- Starks, Laura T, Parth Venkat, and Qifei Zhu.** 2017. “Corporate ESG profiles and investor horizons.” *Available at SSRN 3049943*. 6
- Zerbib, Olivier David.** 2019. “The Effect Of Pro-Environmental Preferences On Bond Prices: Evidence From Green Bonds.” *Journal of Banking & Finance*, 98: 39–60. 5, 6
- Zerbib, Olivier David.** 2022. “A Sustainable Capital Asset Pricing Model (S-CAPM): Evidence from Environmental Integration and Sin Stock Exclusion\*.” *Review of Finance*, 26(6): 1345–1388. 5